Supporting Information

A general concept for the introduction of hydroxamic acids into polymers

Tobias Johann,[a] Jennifer Keth,[a] Matthias Bros [b] and Holger Frey [*,a]

[a.] *Institute of Organic Chemistry, Johannes Gutenberg University, Duesbergweg 10-14, 55124 Mainz, Germany.*
[b.] *Department of Dermatology, University Medical Center of the Johannes Gutenberg University Mainz, Langenbeckstrasse 1, 55131 Mainz, Germany*

Table of contents

Optimization of protected hydroxamic acids with aliphatic spacers 3

SEC and LCST Polymer characterization 3

NMR and IR Characterization 5

Characterization of *N*-hydroxy-4-(2-hydroxyethoxy)benzamide (1b) "HA-OH" 5

Characterization of 2-(4-(5,5-dimethyl-1,4,2-dioxazol-3-yl)phenoxy)ethan-1-ol (1c) "HAA-OH" 8

Characterization of N,4-dihydroxybenzamide (2a) 11

Characterization of 4-(5,5-dimethyl-1,4,2-dioxazol-3-yl)phenol (2b) 14

Characterization of *N*-hydroxy-4-(hydroxymethyl)benzamide (3a) 17

Characterization of (4-(5,5-dimethyl-1,4,2-dioxazol-3-yl)phenyl)methanol (3b) ^{benzyl}HAA-OH 20

Characterization of *N*,6-dihydroxyhexanamide (4a) 23

Characterization of 5-(5,5-dimethyl-1,4,2-dioxazol-3-yl)pentan-1-ol (4b) 26

Characterization of 5,5-dimethyl-3-(4-(2-(oxiran-2-ylmethoxy)ethoxy)phenyl) -1,4,2-dioxazole (1d) 27

Characterization of 2-(4-(5,5-dimethyl-1,4,2-dioxazol-3-yl)phenoxy)ethyl methacrylate (1e) 27

Characterization of HAA-PEG (P1a), HA-PEG (P1b) and ^{benzyl}HAA-PEG (P2a) polymers 28

Characterization of HAA-PPO (P3a), ^{benzyl}HAA-PPO (P4a), HAA-PEEGE (P5a) and ^{benzyl}HAA-PEEGE (P6a) polymers 29

Polymer mass spectroscopy characterization 31

Complexation properties 32

Nanoparticle characterization 33

T-Cell proliferation assay and MTT metabolic activity analysis 34

Optimization of protected hydroxamic acids with aliphatic spacers

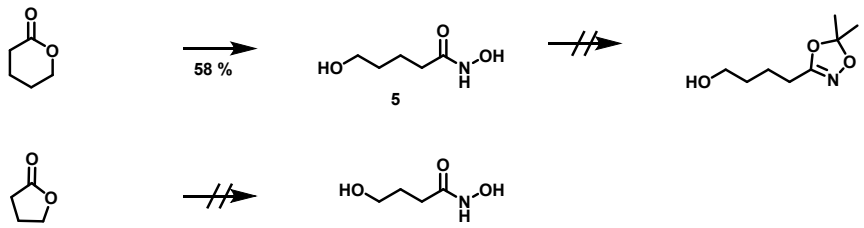

Scheme S1. Overview over the synthesis attempts to yield protected hydroxamic acids with C_4 and C_3 aliphatic spacers.

SEC and LCST Polymer characterization

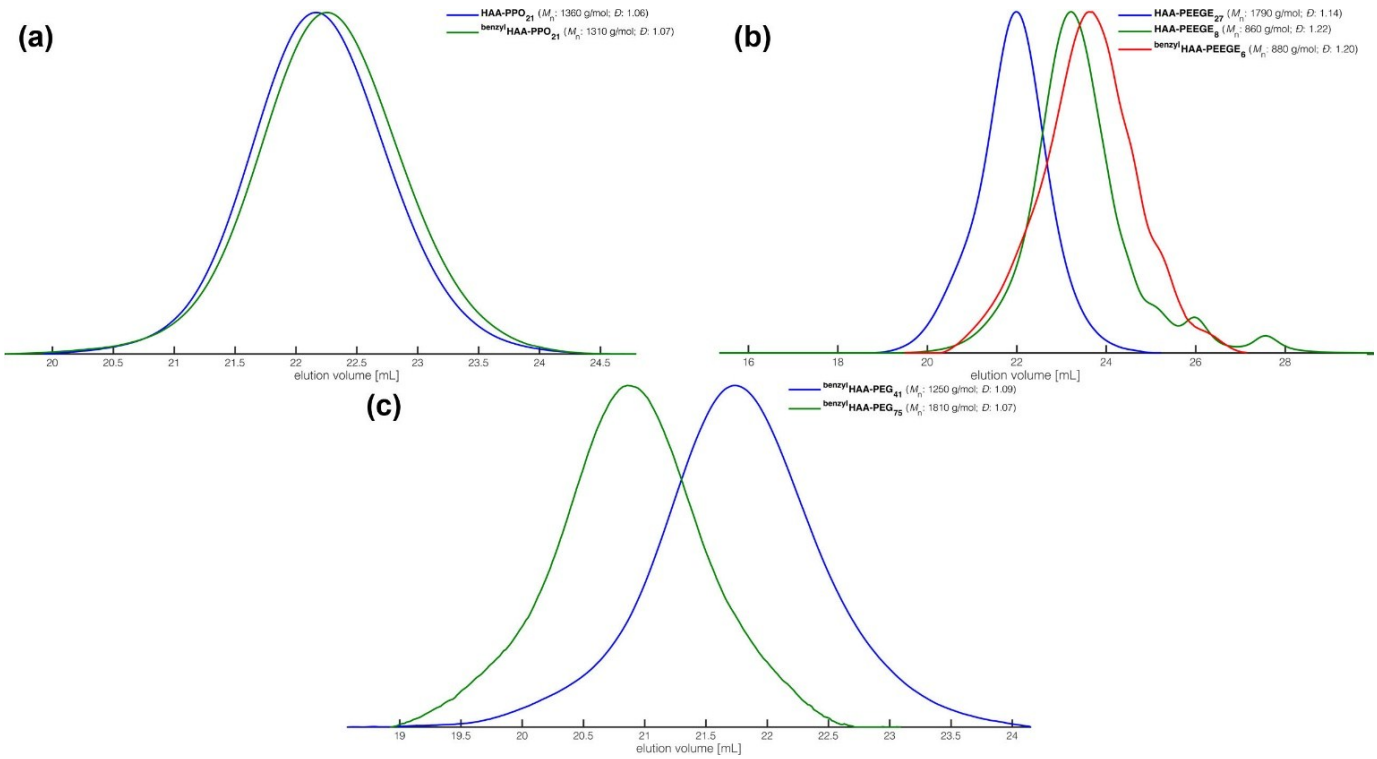

Figure S1. (a) SEC traces of PPO polymers. (b) SEC traces of PEEGE polymer. (c) ^{benzyl}HAA-PEG polymers.

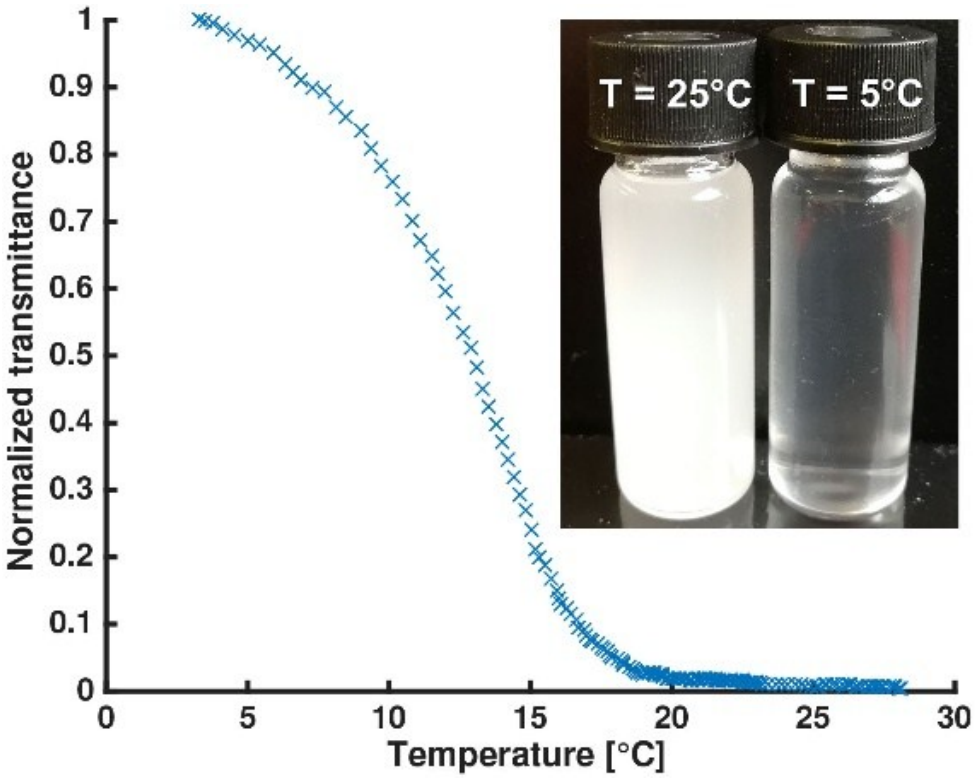

Figure S2. Cloud point measurement of HAA-PPO_{21} in deionized water. Turbidity rapidly increased between 10 and 15 °C with 50 % of original transmittance at 12.9°C.

NMR and IR Characterization

Characterization of *N*-hydroxy-4-(2-hydroxyethoxy)benzamide (1b) "HA-OH"

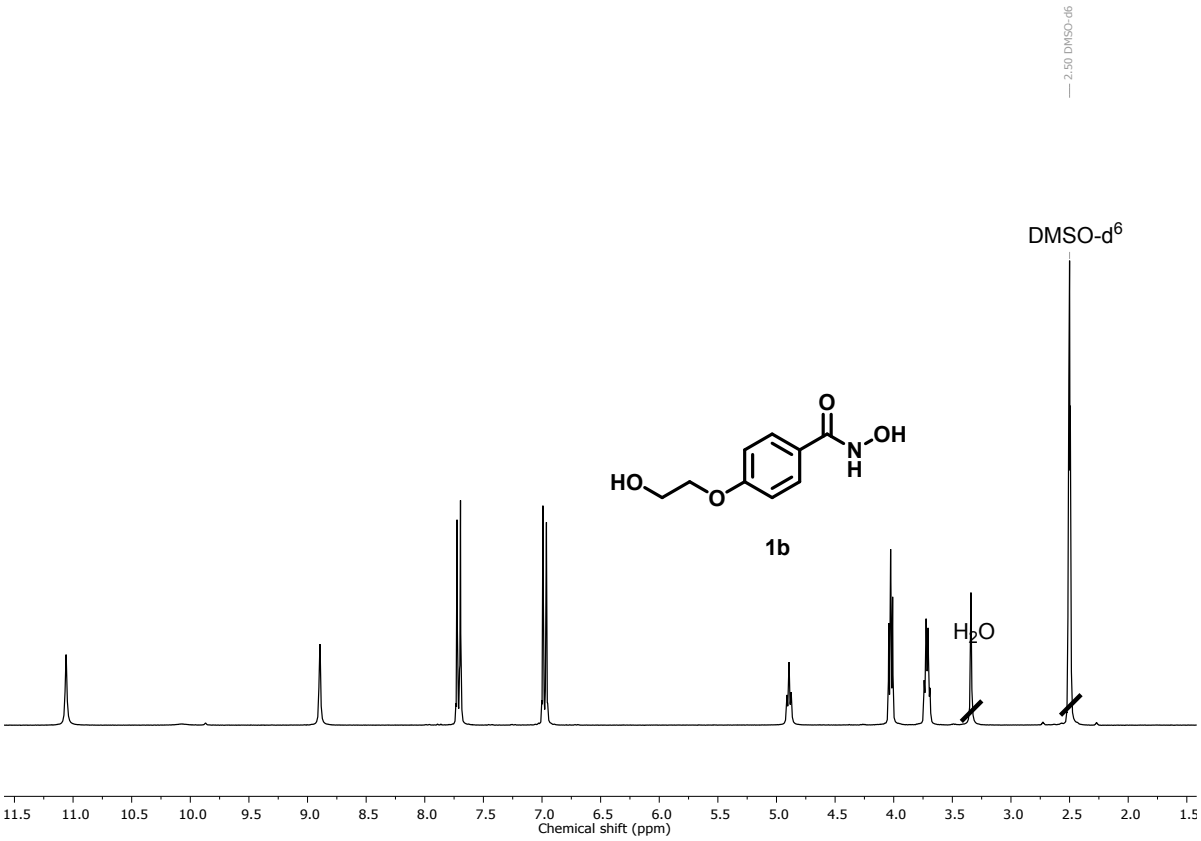

Figure S3a. ^{1}H NMR spectrum (300 MHz, DMSO-d_6) of *N*-hydroxy-4-(2-hydroxyethoxy)benzamide **(1b)**. See synthesis procedure for detailed assignment of the signals.

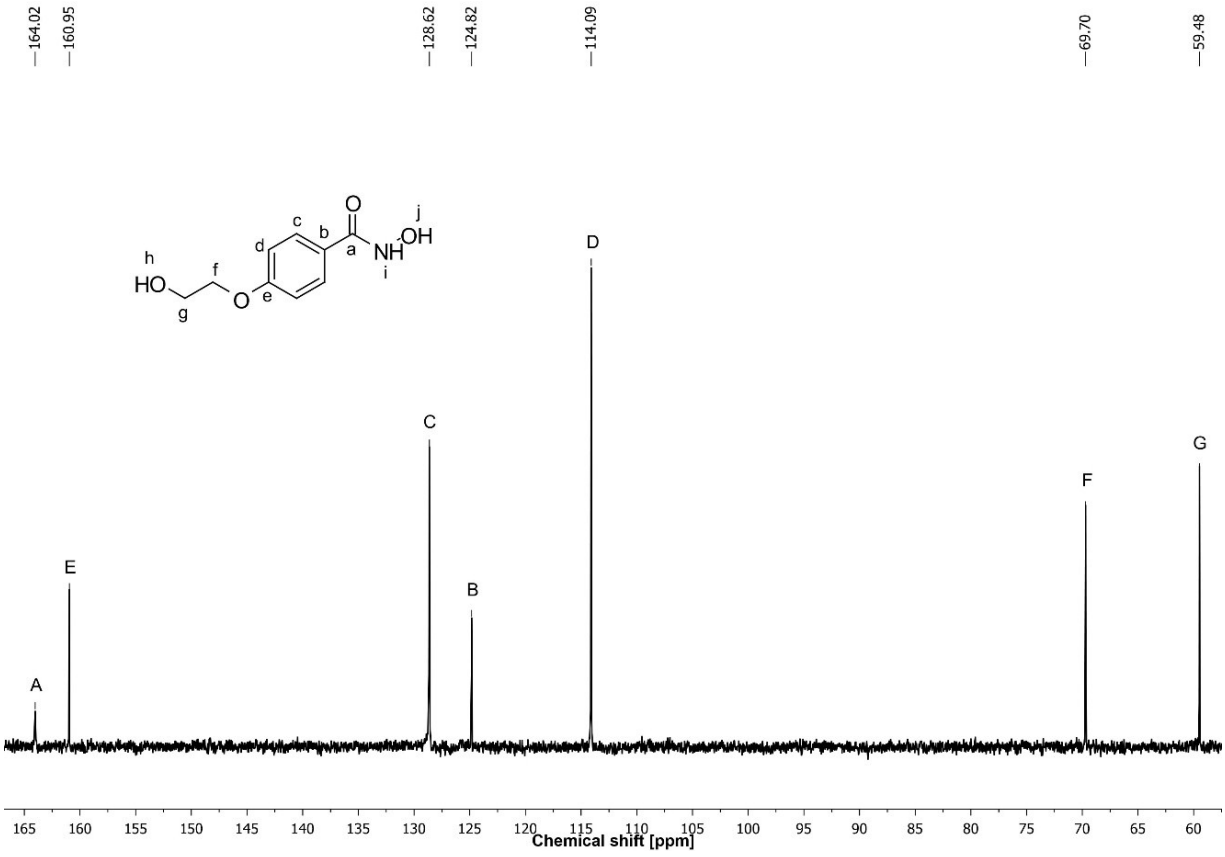

Figure S3b. ^{13}C NMR spectrum (75 MHz, DMSO-d_6) of *N*-hydroxy-4-(2-hydroxyethoxy)benzamide **(1b)**.

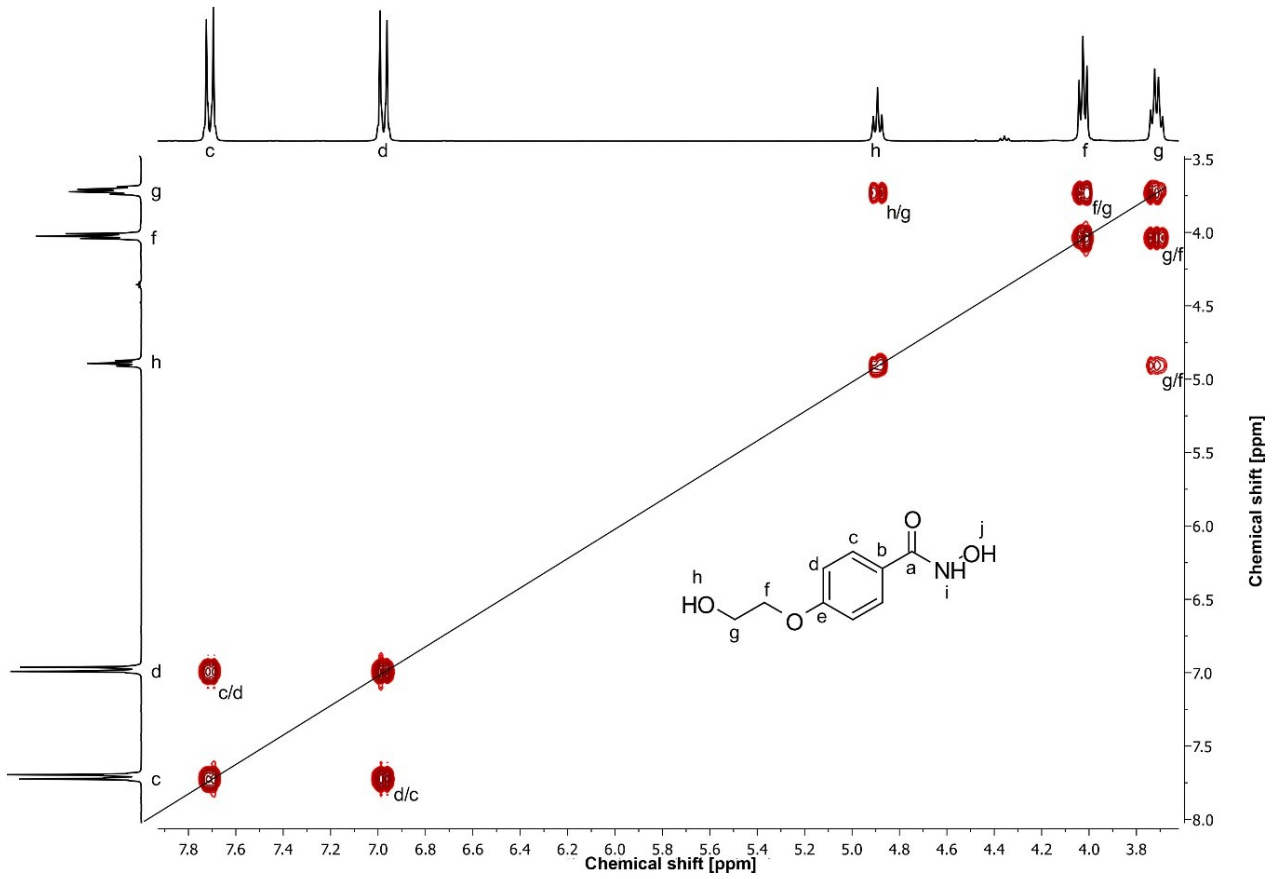

Figure S3c. ^{1}H-^{1}H COSY NMR spectrum (300 MHz, DMSO-d_6) of *N*-hydroxy-4-(2-hydroxyethoxy)benzamide **(1b)**.

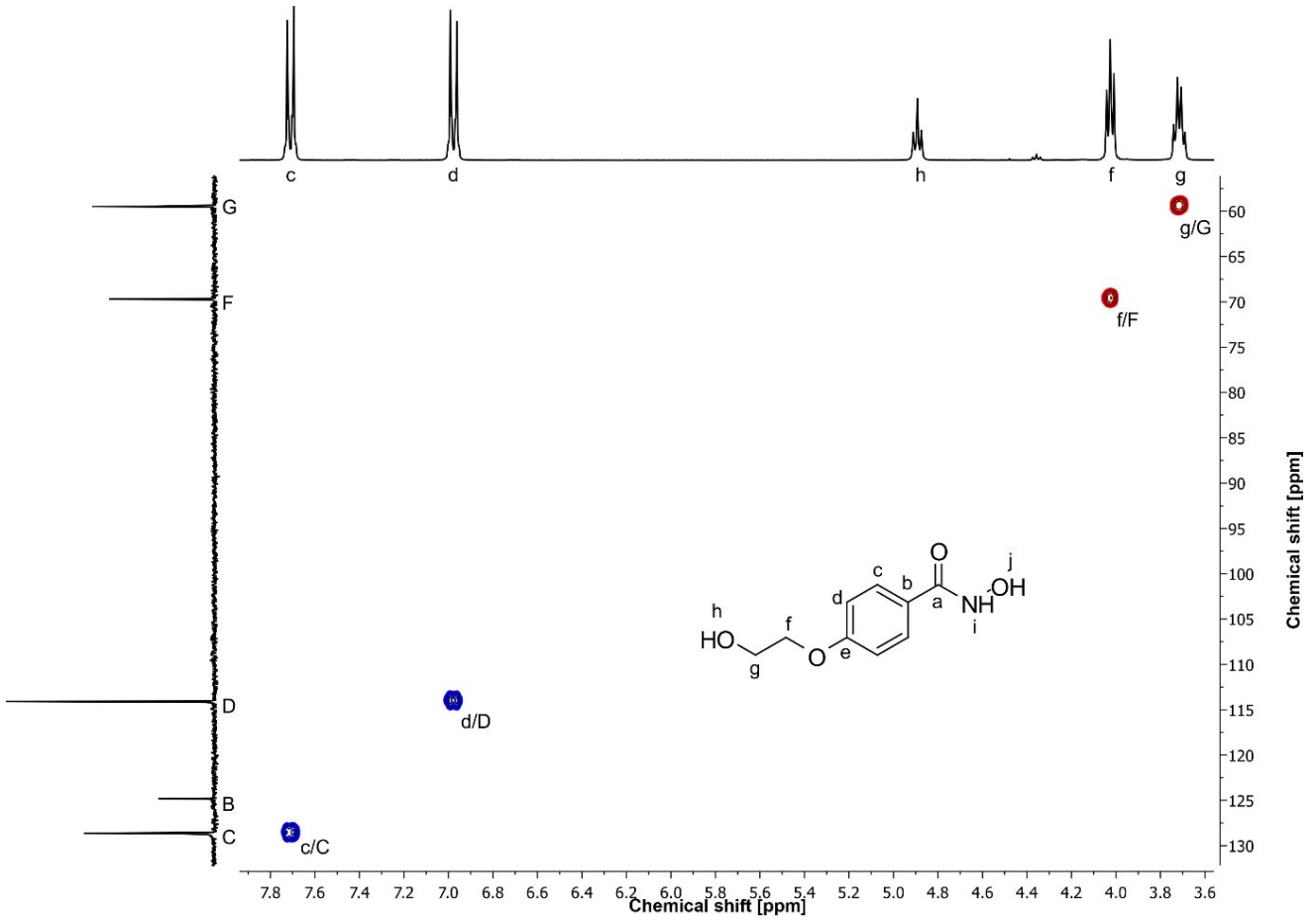

Figure S3d. ^{1}H-^{13}C HSQC NMR spectrum (300 MHz / 75 MHz, DMSO-d_6) of *N*-hydroxy-4-(2-hydroxyethoxy)benzamide (**1b**).

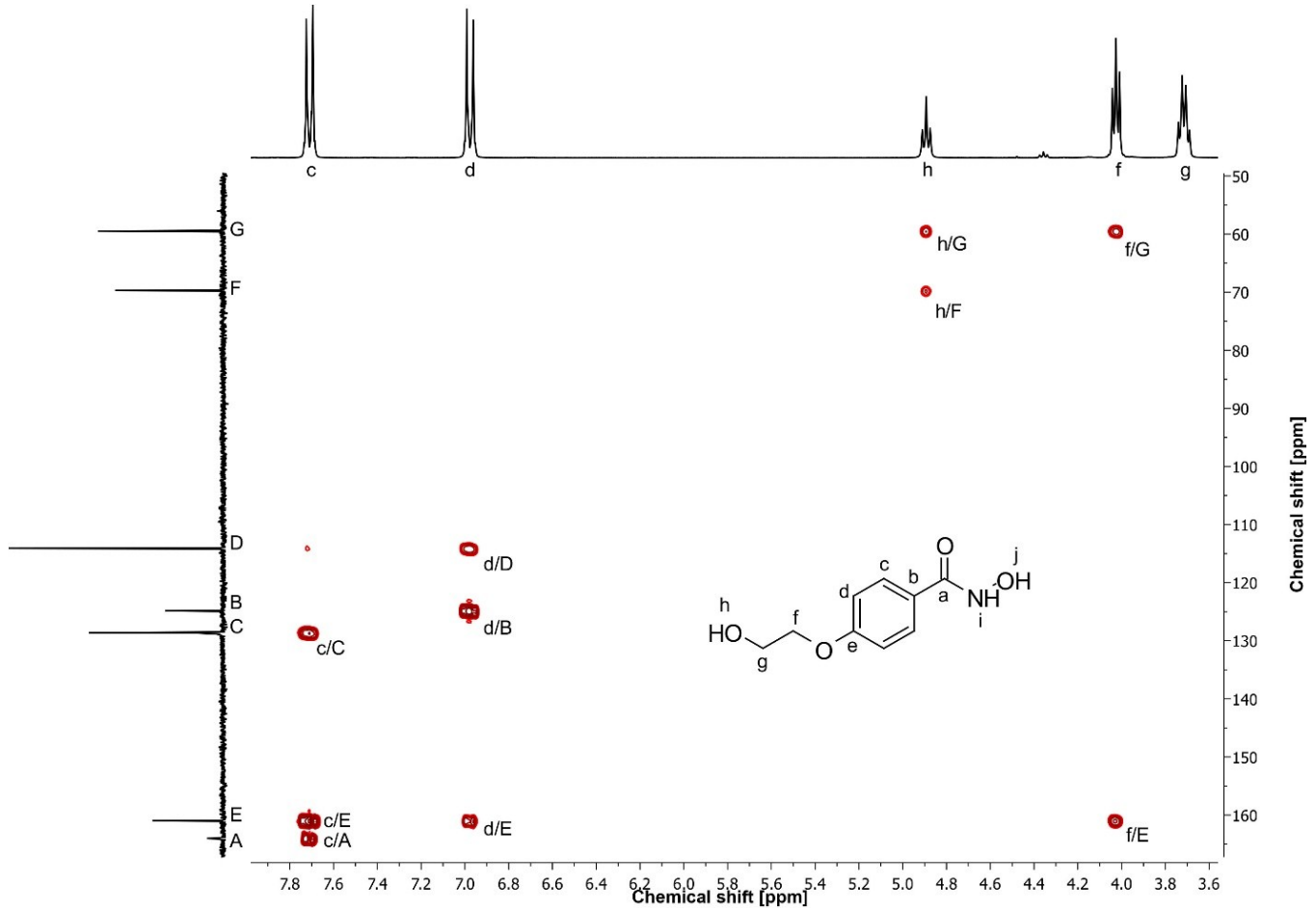

Figure S3e. ^{1}H-^{13}C HMBC NMR spectrum (300 MHz / 75 MHz, DMSO-d_6) of *N*-hydroxy-4-(2-hydroxyethoxy)benzamide **(1b).**

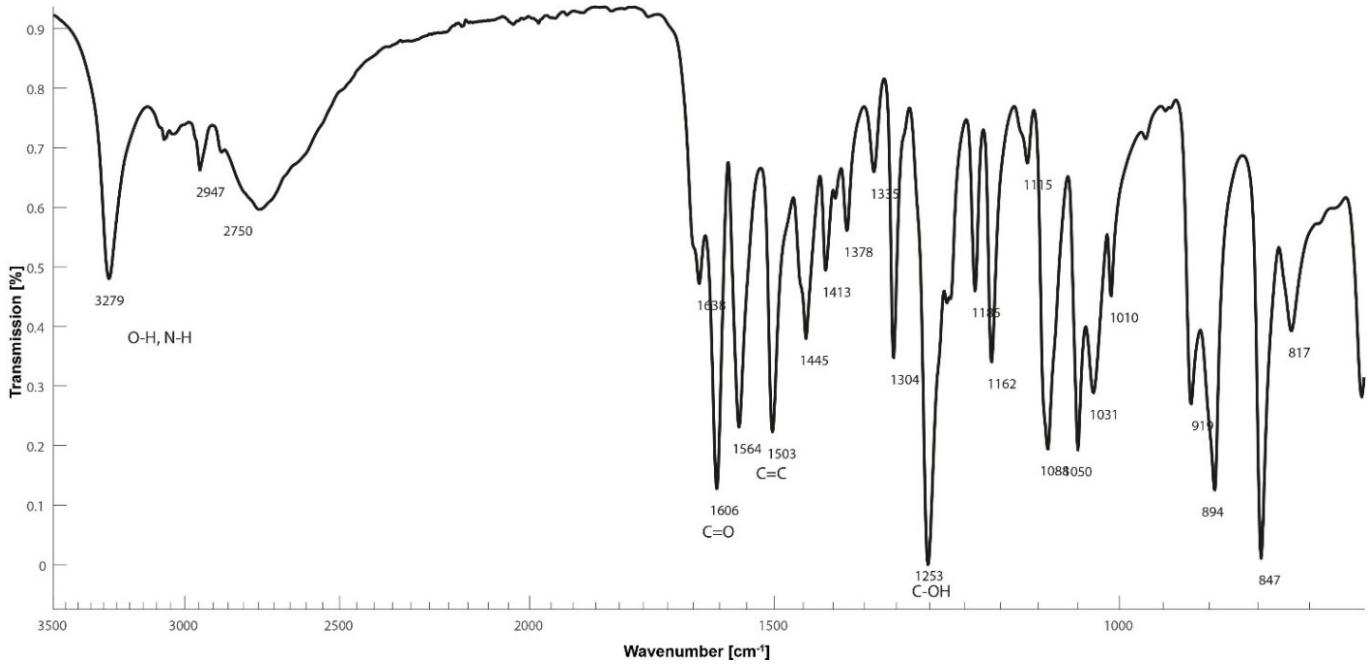

Figure S3f. FT-ATR-IR spectrum of *N*-hydroxy-4-(2-hydroxyethoxy)benzamide **(1b).**

Characterization of 2-(4-(5,5-dimethyl-1,4,2-dioxazol-3-yl)phenoxy)ethan-1-ol (1c) "HAA-OH"

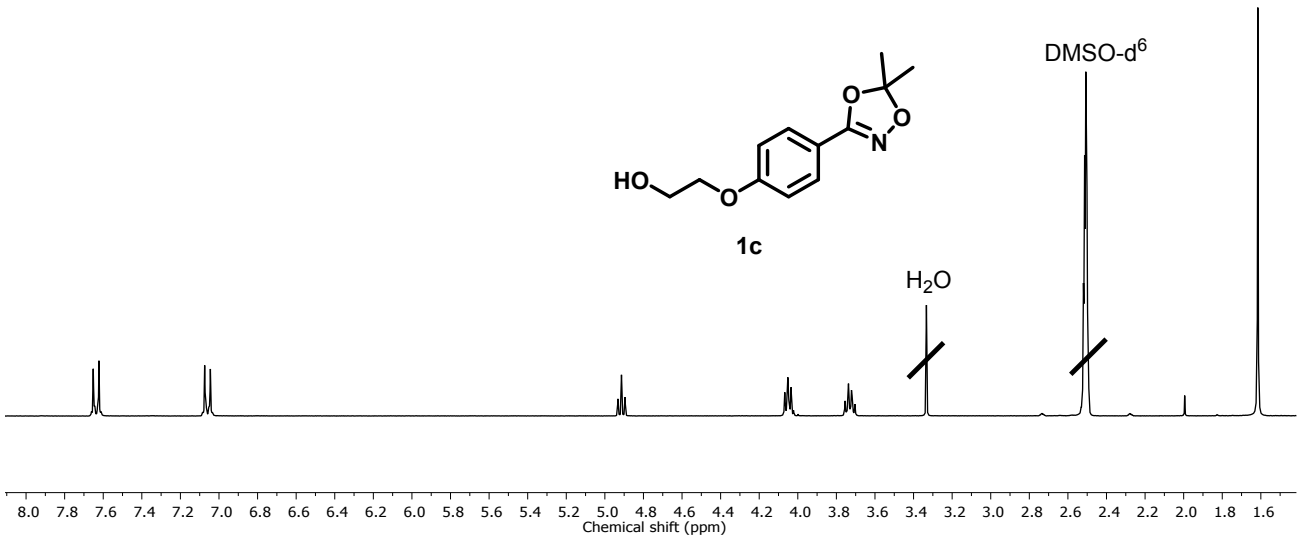

Figure S4a. ^{1}H NMR spectrum (300 MHz, DMSO-d_6) of 2-(4-(5,5-dimethyl-1,4,2-dioxazol-3-yl)phenoxy)ethan-1-ol **(1c).** See synthesis procedure for detailed assignment of the signals.

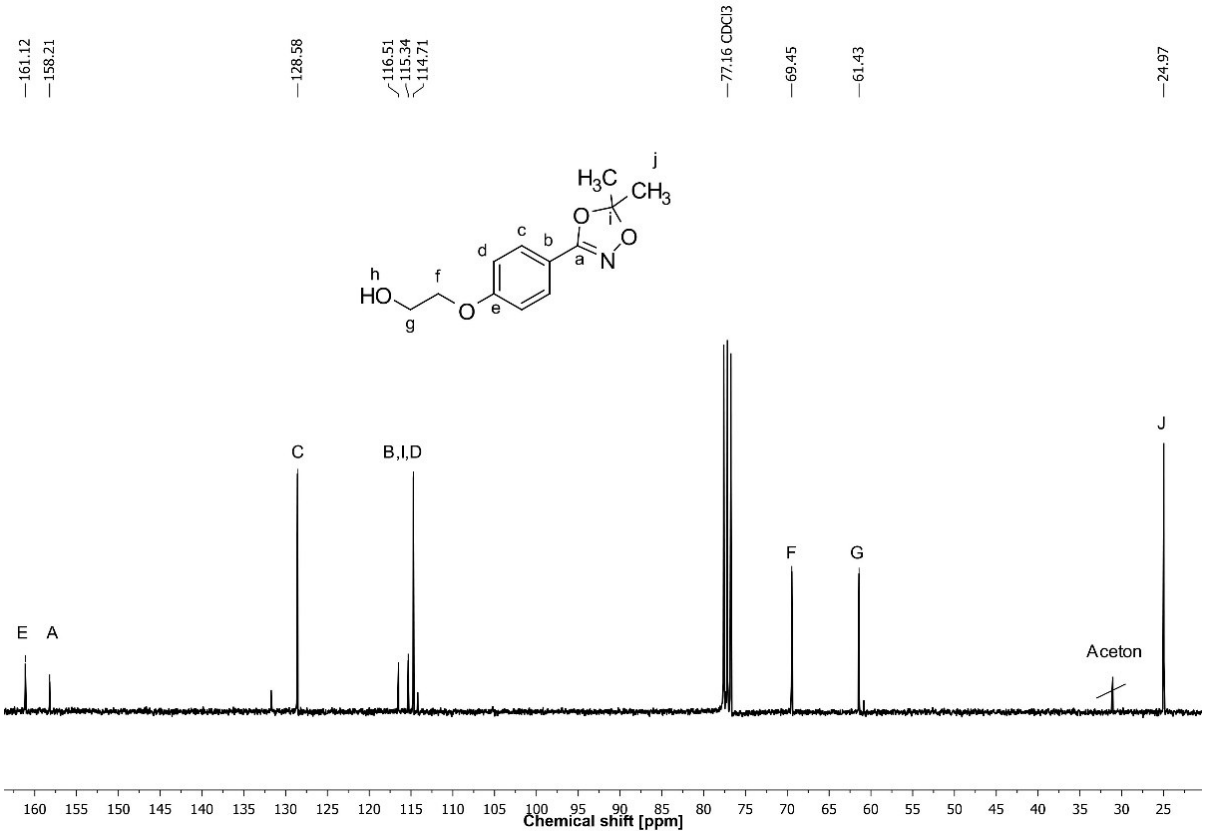

Figure S4b. ^{13}C NMR spetrcum (75 MHz, DMSO-d_6) of 2-(4-(5,5-dimethyl-1,4,2-dioxazol-3-yl)phenoxy)ethan-1-ol **(1c)** prior to purification via column chromatography.

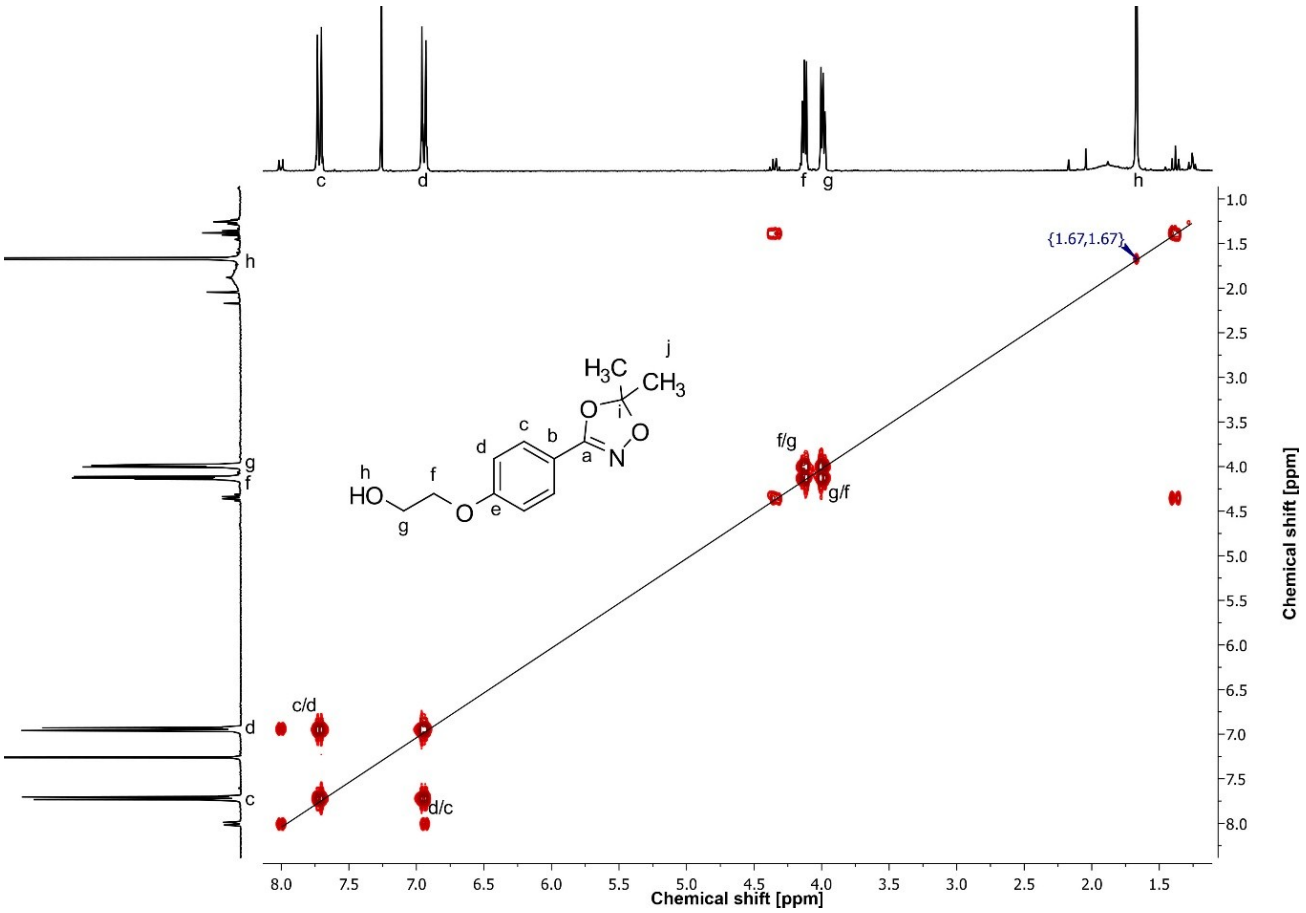

Figure S4c. ^{1}H-^{1}H COSY NMR spetrum (300 MHz, DMSO-d_6) of 2-(4-(5,5-dimethyl-1,4,2-dioxazol-3-yl)phenoxy)ethan-1-ol **(1c)** prior to purification via column chromatography.

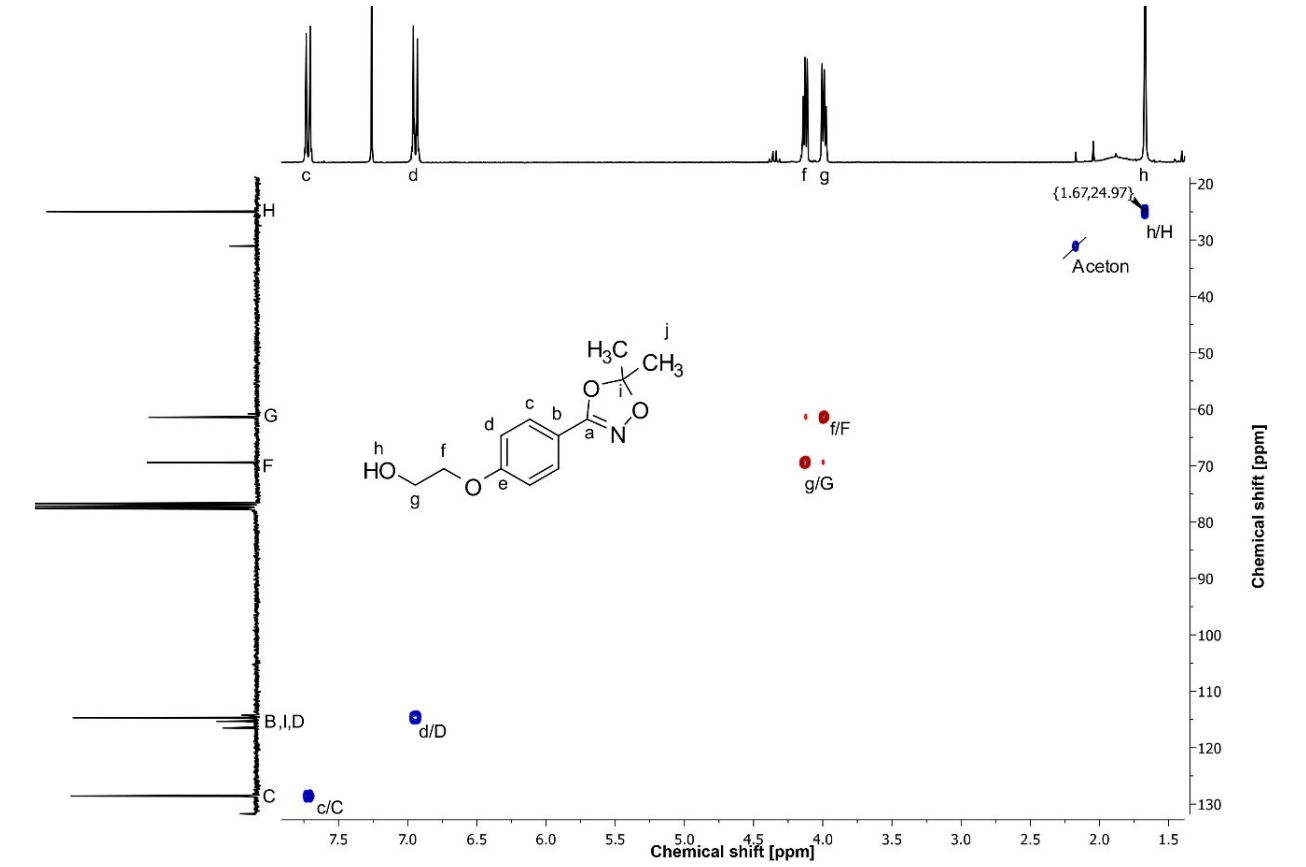

Figure S4d. ^{1}H-^{13}C HSQC NMR spectrum (300 MHz / 75 MHz, DMSO-d_6) of 2-(4-(5,5-dimethyl-1,4,2-dioxazol-3-yl)phenoxy)ethan-1-ol **(1c)** prior to purification via column chromatography.

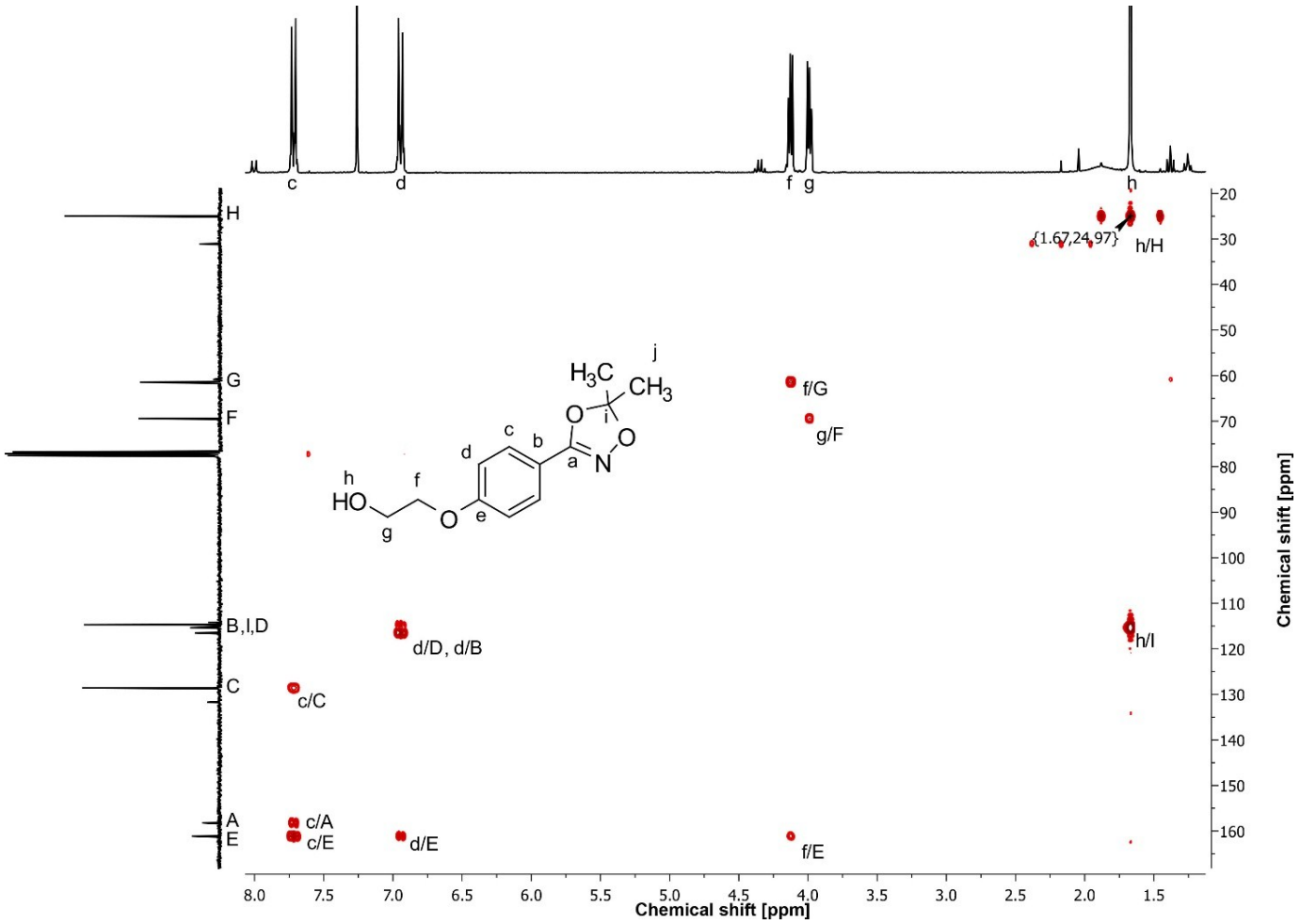

Figure S4e. ^{1}H-^{13}C HMBC NMR spectrum (300 MHz / 75 MHz, DMSO-d_6) of 2-(4-(5,5-dimethyl-1,4,2-dioxazol-3-yl)phenoxy)ethan-1-ol **(1c)** prior to purification via column chromatography.

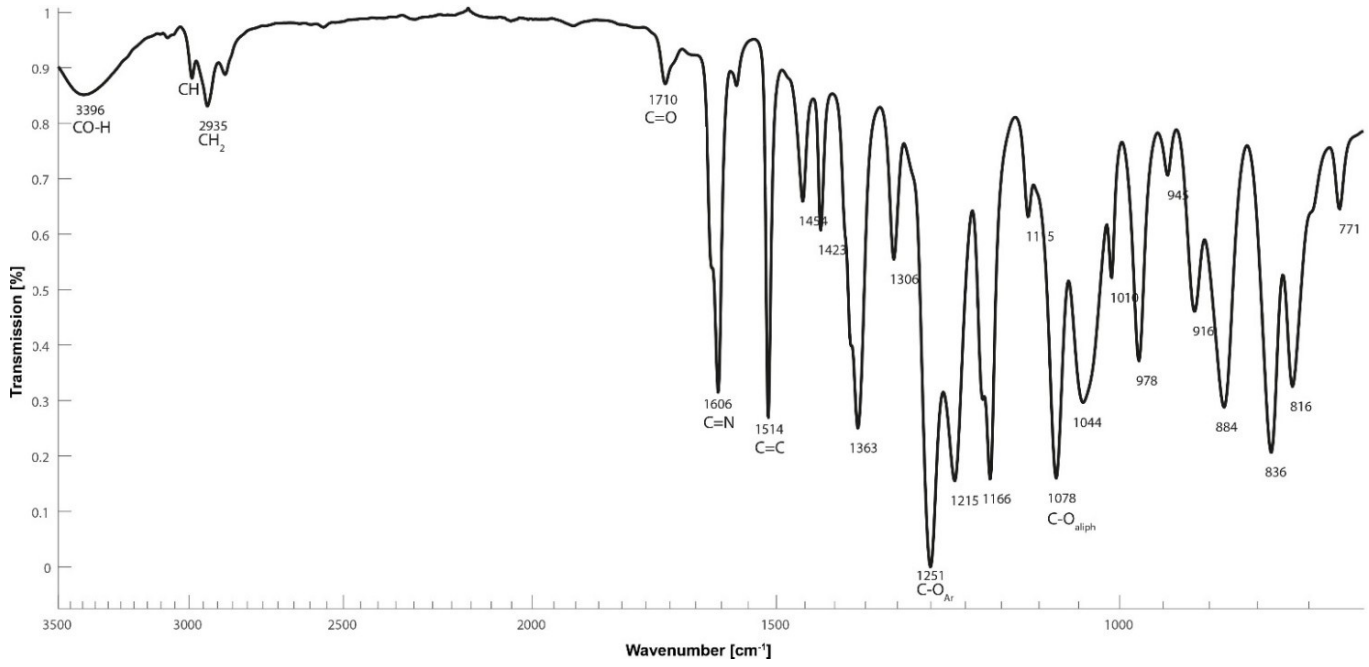

Figure S4f. FT-ATR-IR spectrum of 2-(4-(5,5-dimethyl-1,4,2-dioxazol-3-yl)phenoxy)ethan-1-ol **(1c)** prior to purification via column chromatography.

Characterization of *N*,4-dihydroxybenzamide (2a)

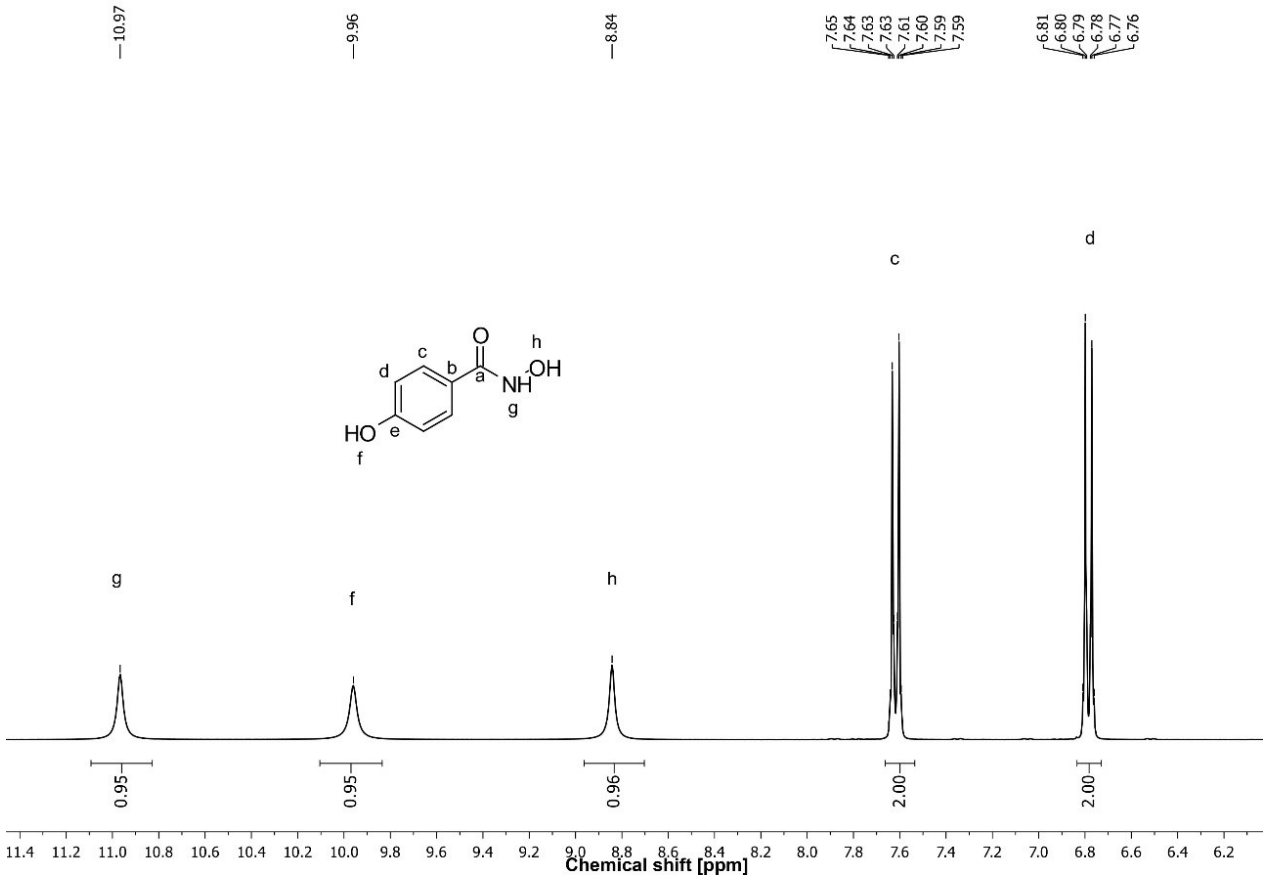

Figure S5a. ^{1}H NMR spectrum (300 MHz, DMSO-d_6) of *N*,4-dihydroxybenzamide **(2a).**

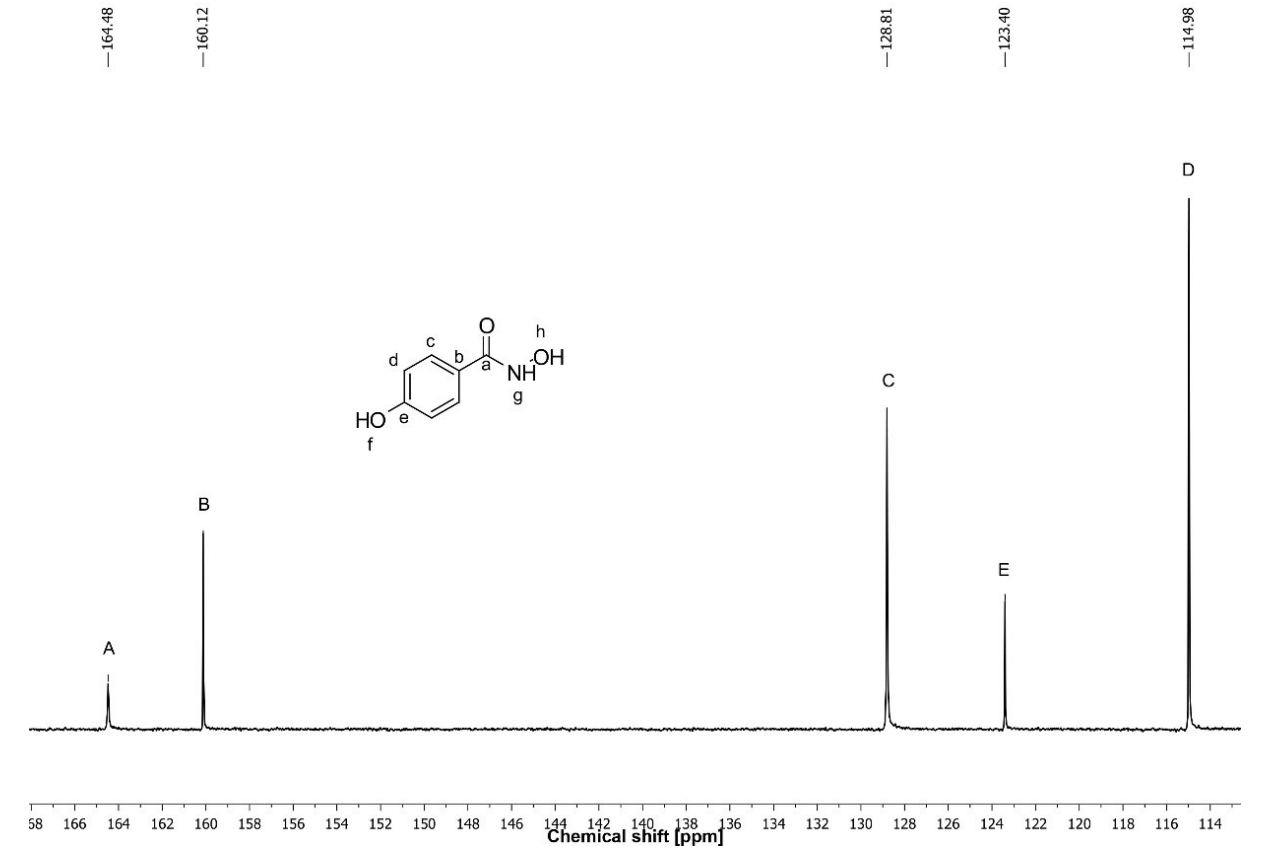

Figure S5b. ^{13}C NMR spectrum (75 MHz, DMSO-d_6) of *N*,4-dihydroxybenzamide **(2a).**

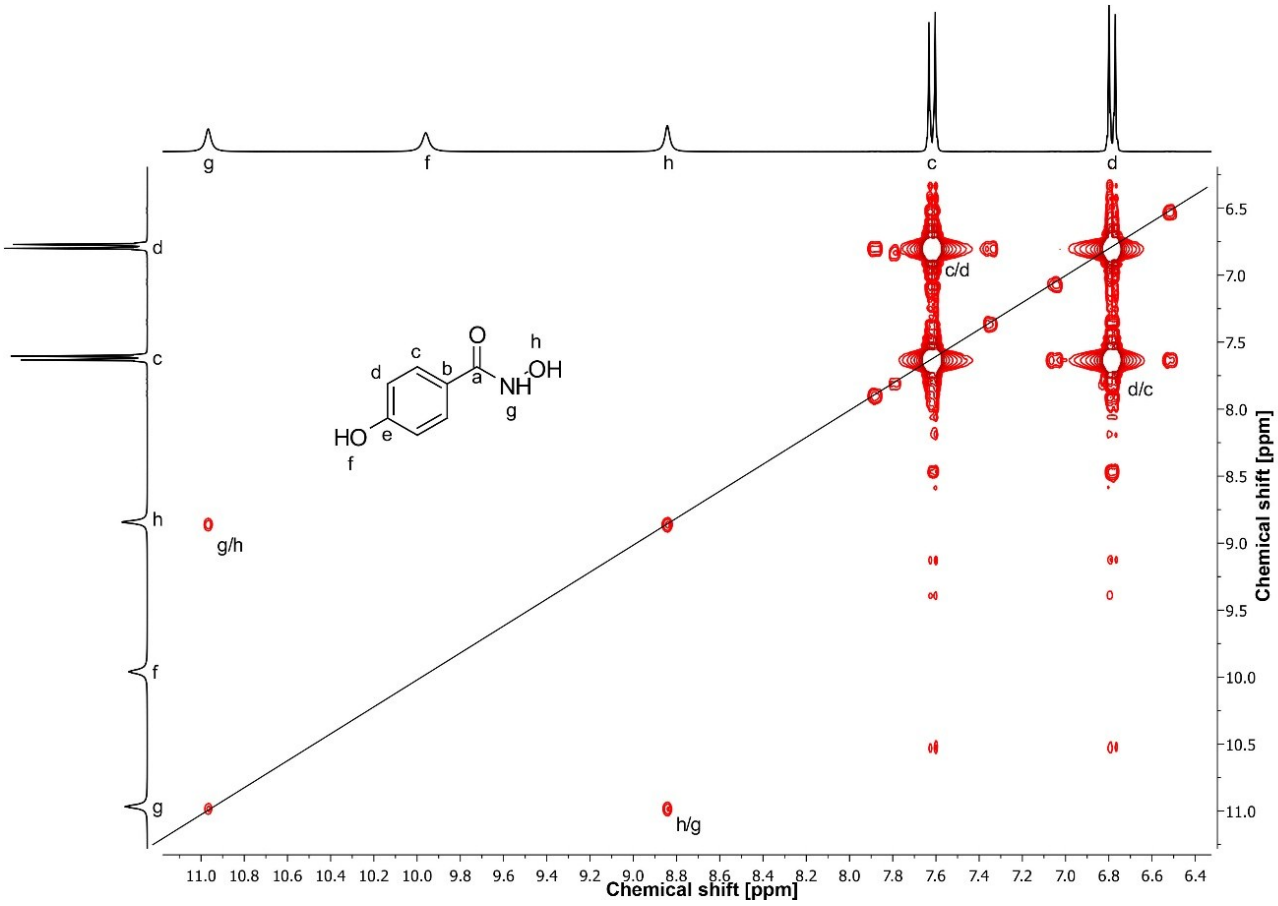

Figure S5c. ^{1}H-^{1}H COSY NMR spectrum (300 MHz, DMSO-d_6) of *N*,4-dihydroxybenzamide **(2a).**

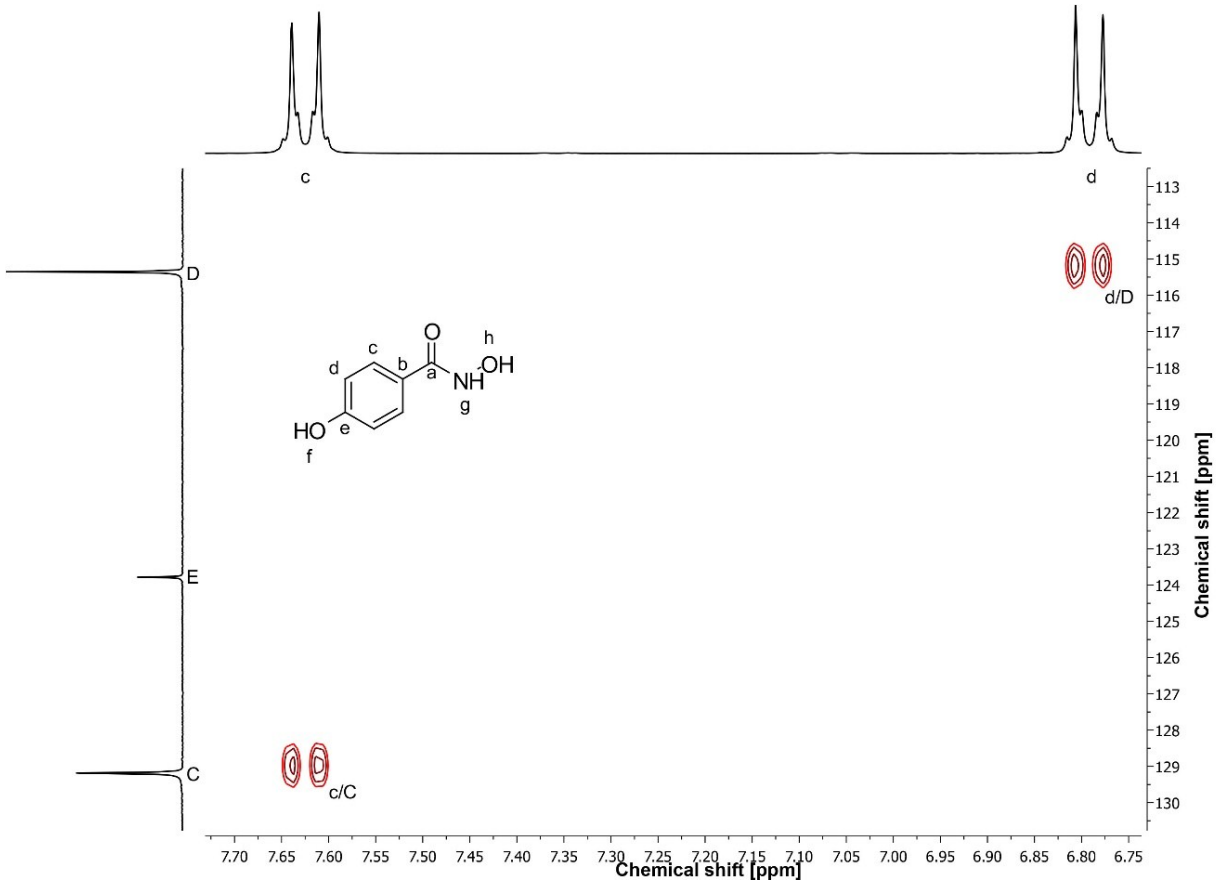

Figure S5d. ^{1}H-^{13}C HSQC NMR spectrum (300 MHz / 75 MHz, DMSO-d_6) of *N*,4-dihydroxybenzamide **(2a).**

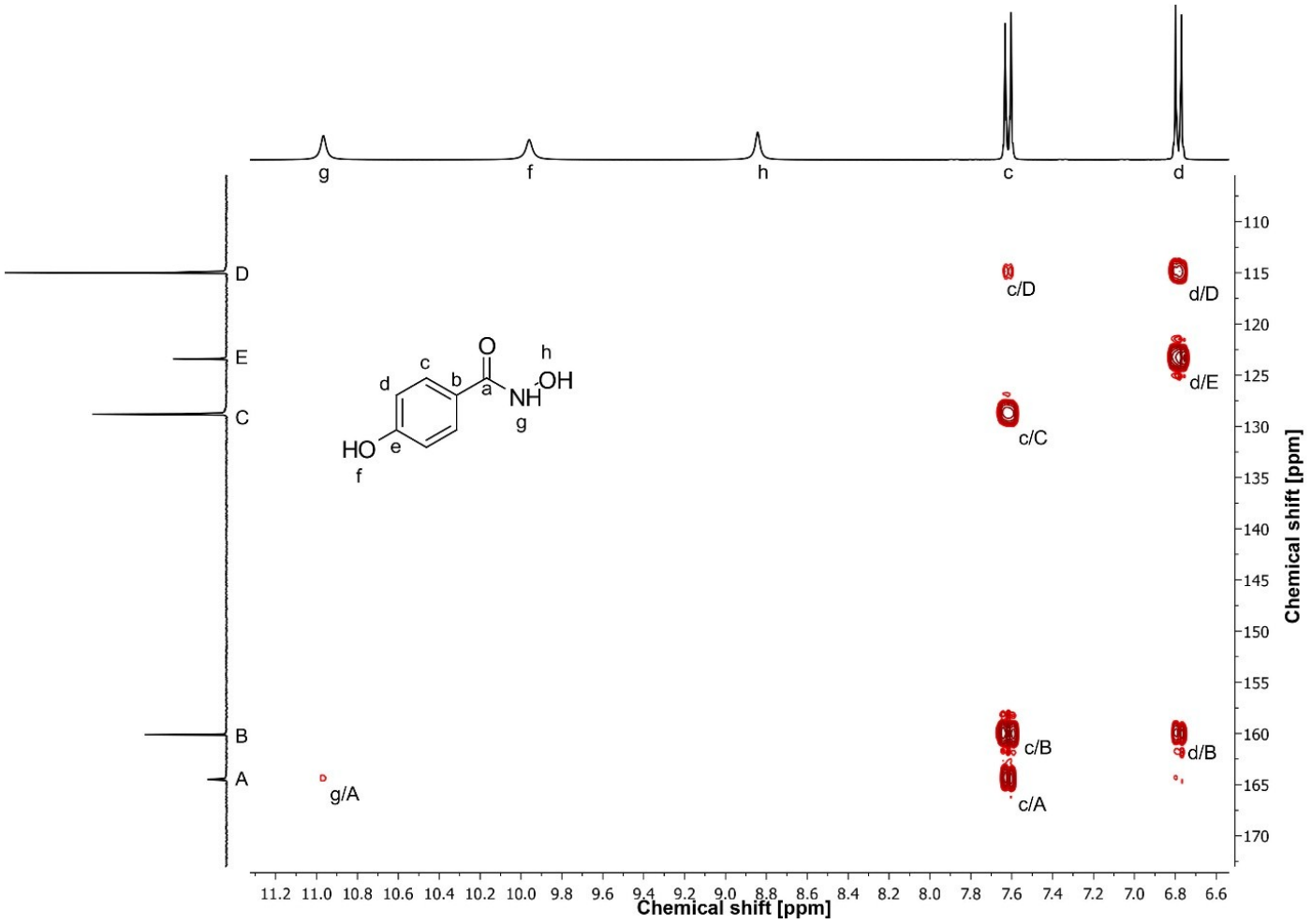

Figure S5e. ^{1}H-^{13}C HMBC NMR spectrum (300 MHz / 75 MHz, DMSO-d_6) of *N*,4-dihydroxybenzamide **(2a).**

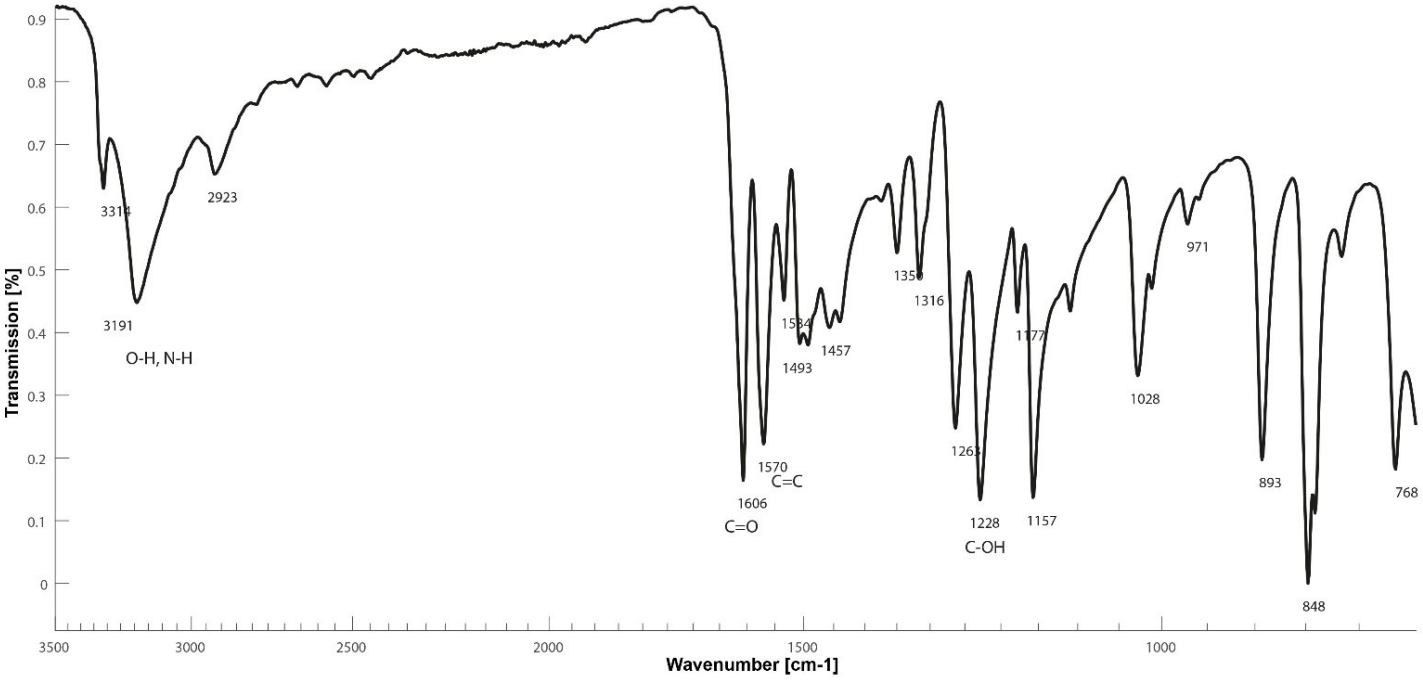

Figure S5f. FT-ATR-IR spectrum of *N*,4-dihydroxybenzamide **(2a).**

Characterization of 4-(5,5-dimethyl-1,4,2-dioxazol-3-yl)phenol (2b)

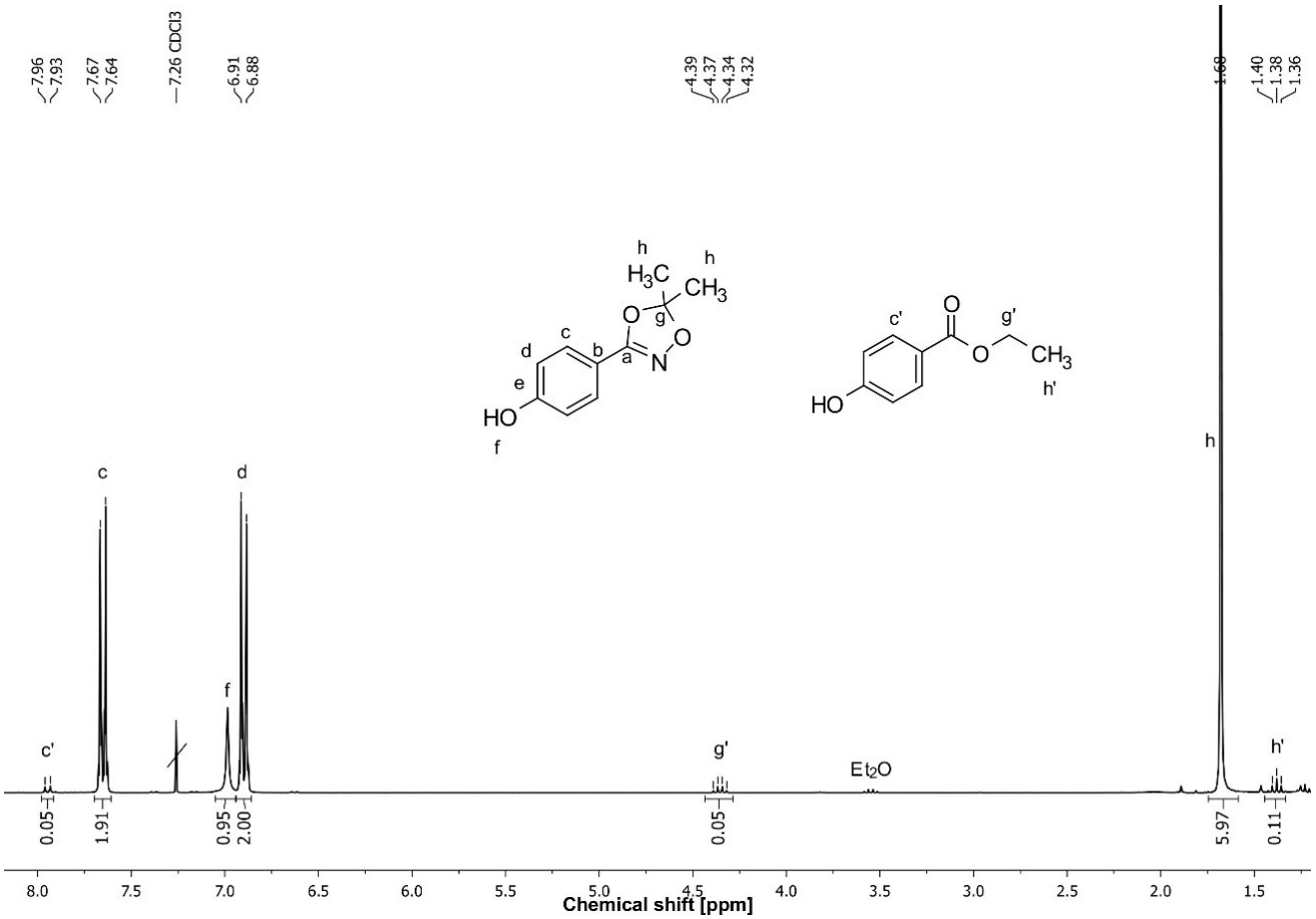

Figure S6a. ^{1}H NMR spectrum (300 MHz, DMSO-d_6) of 4-(5,5-dimethyl-1,4,2-dioxazol-3-yl)phenol **(2b).** The ethyl ester residue originates from the side reaction during transketalization.

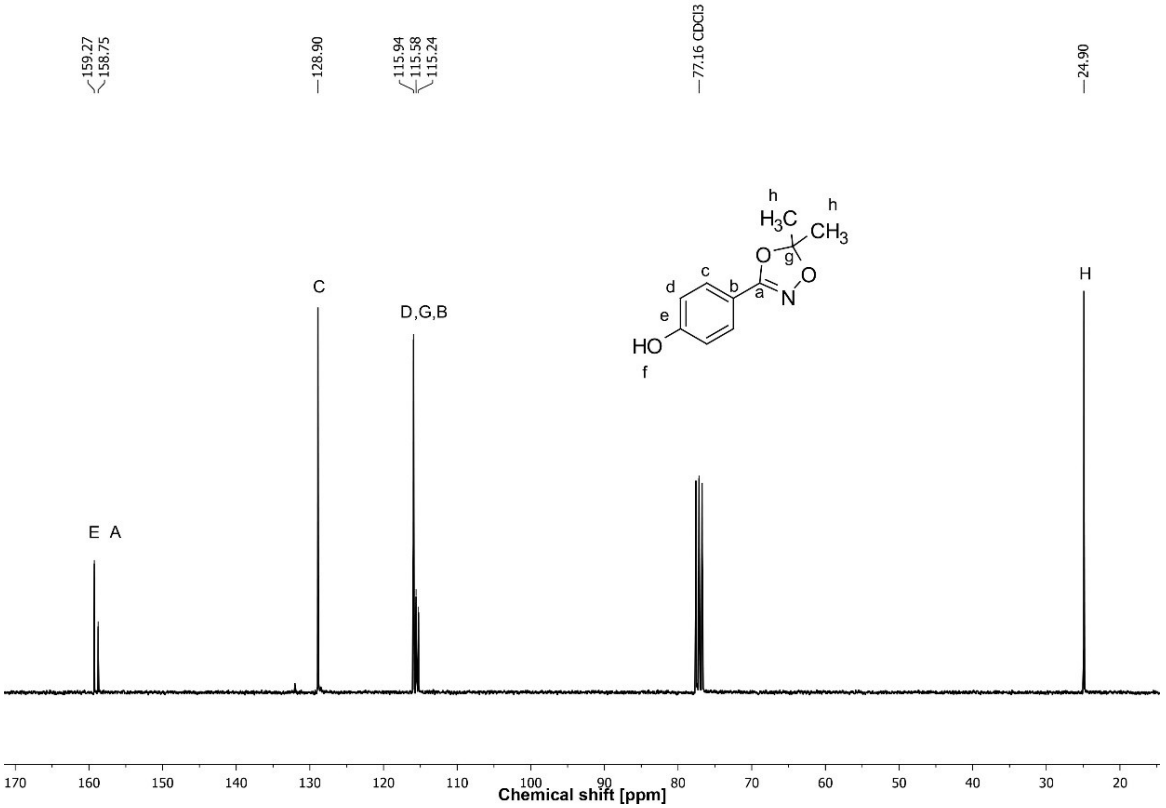

Figure S6b. ^{13}C NMR spectrum (75 MHz, DMSO-d_6) of 4-(5,5-dimethyl-1,4,2-dioxazol-3-yl)phenol **(2b).**

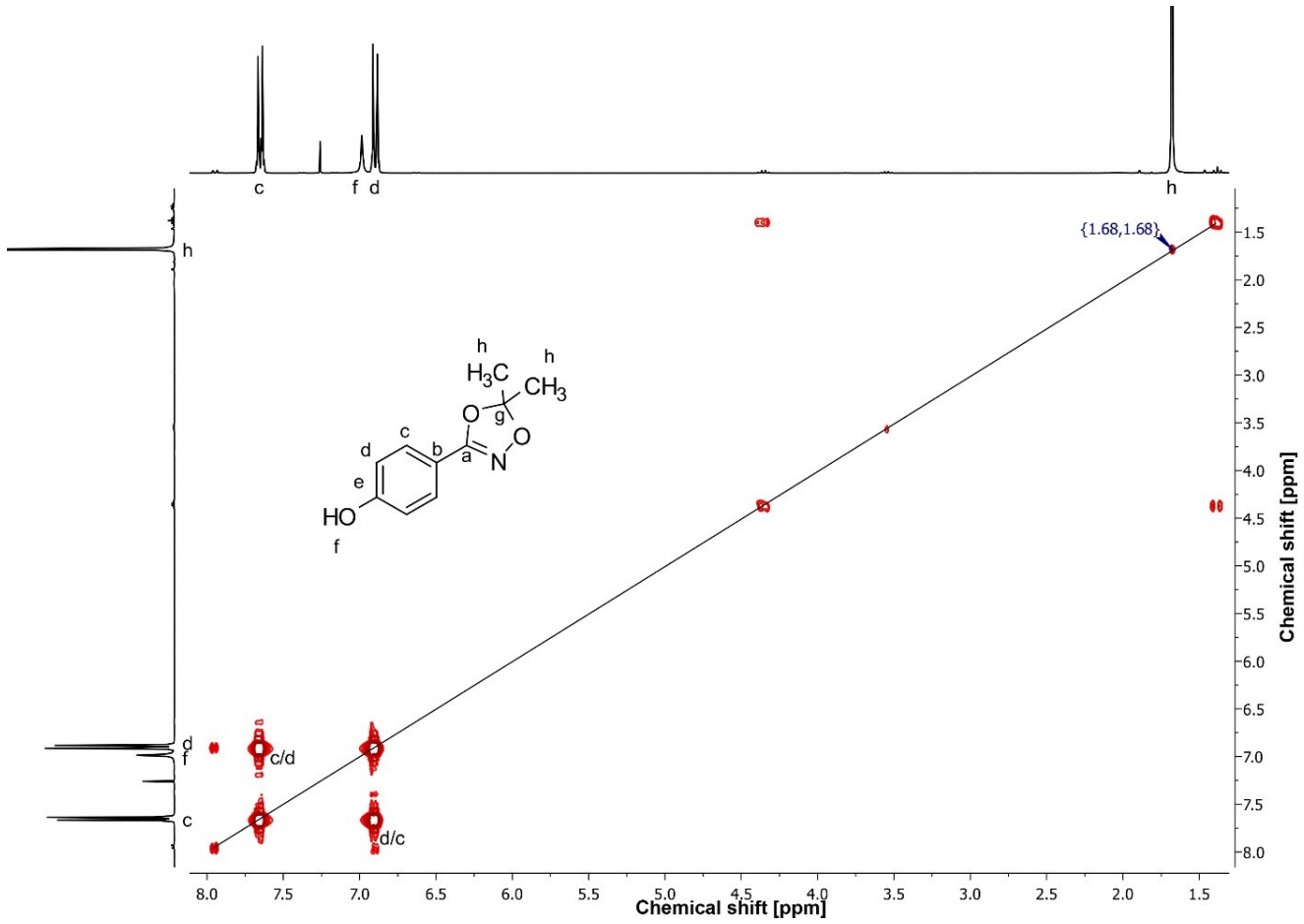

Figure S6c. ^{1}H-^{1}H COSY NMR spectrum (300 MHz, DMSO-d_6) of 4-(5,5-dimethyl-1,4,2-dioxazol-3-yl)phenol **(2b).**

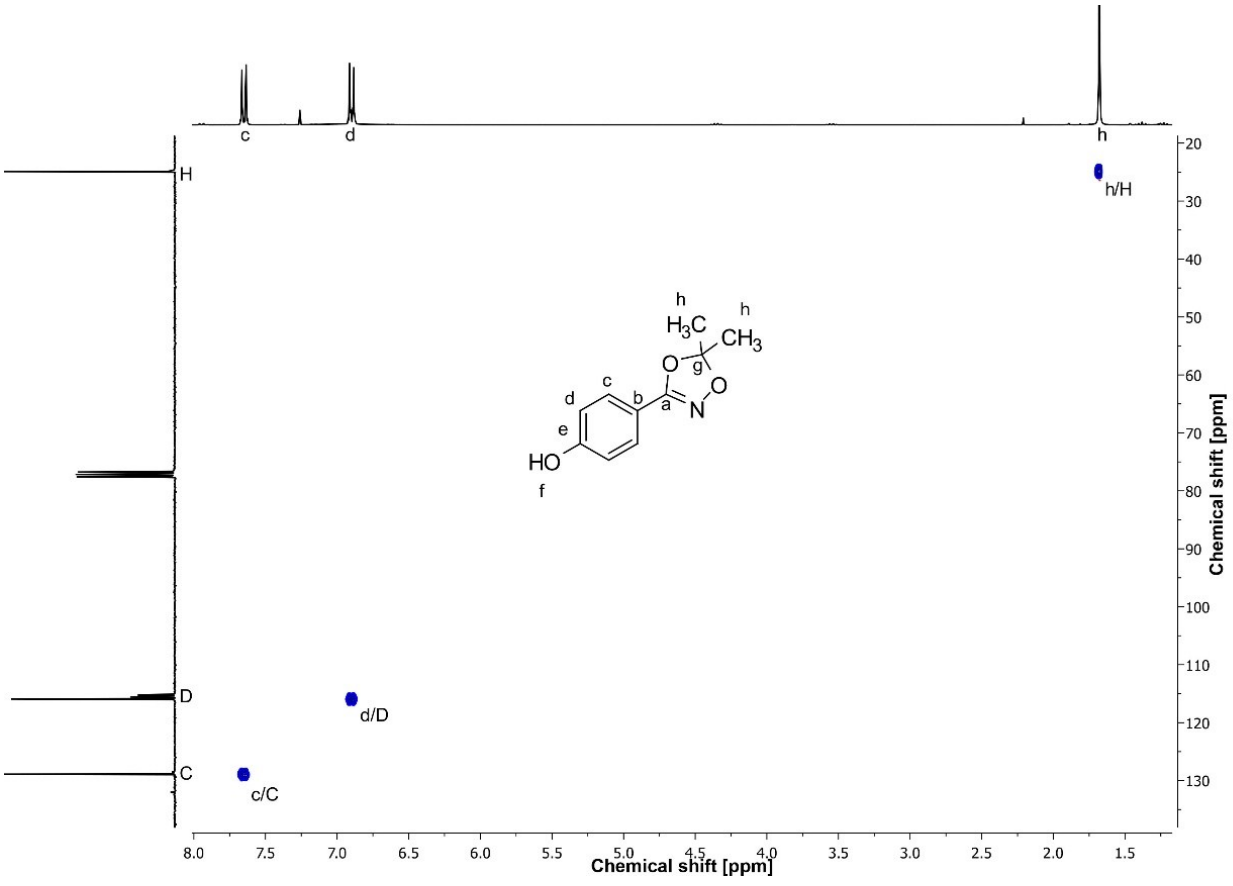

Figure S6d. ^{1}H-^{13}C HSQC NMR spectrum (300 MHz / 75 MHz, DMSO-d_6) of 4-(5,5-dimethyl-1,4,2-dioxazol-3-yl)phenol **(2b).**

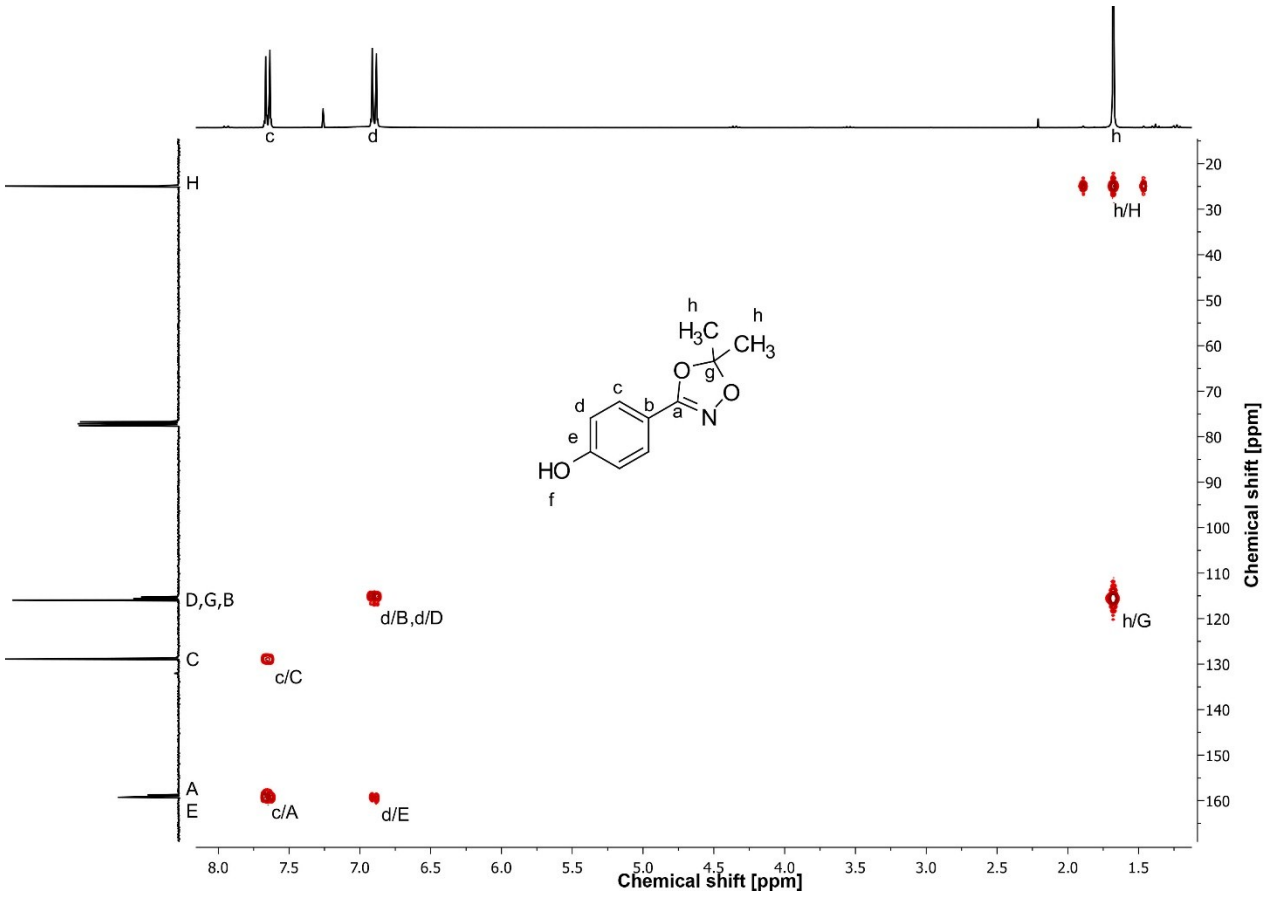

Figure S6e. ^{1}H-^{13}C HMBC NMR spectrum (300 MHz / 75 MHz, DMSO-d_6) of 4-(5,5-dimethyl-1,4,2-dioxazol-3-yl)phenol **(2b).**

Characterization of *N*-hydroxy-4-(hydroxymethyl)benzamide (3a)

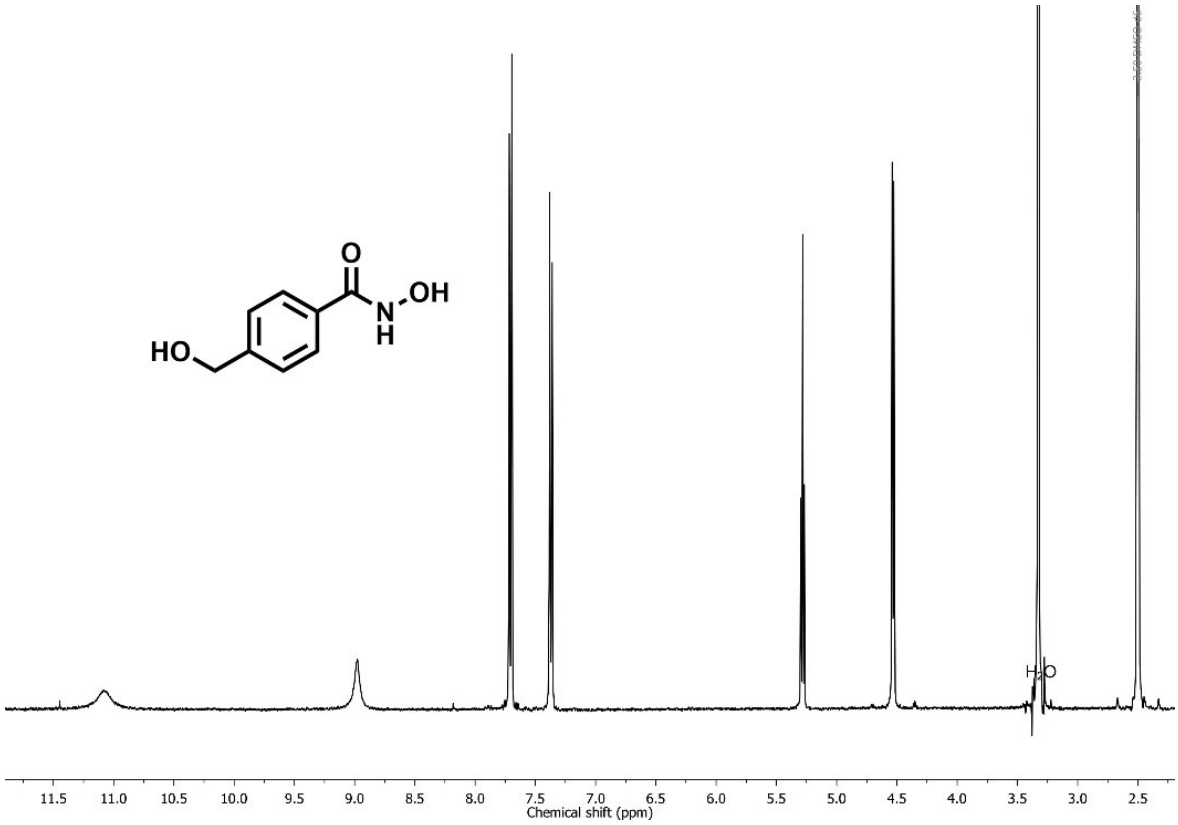

Figure S7a. ^{1}H NMR spectrum (400 MHz, DMSO-d_6) of *N*-hydroxy-4-(hydroxymethyl)benzamide **(3a).** See synthesis procedure for detailed assignment of the signals.

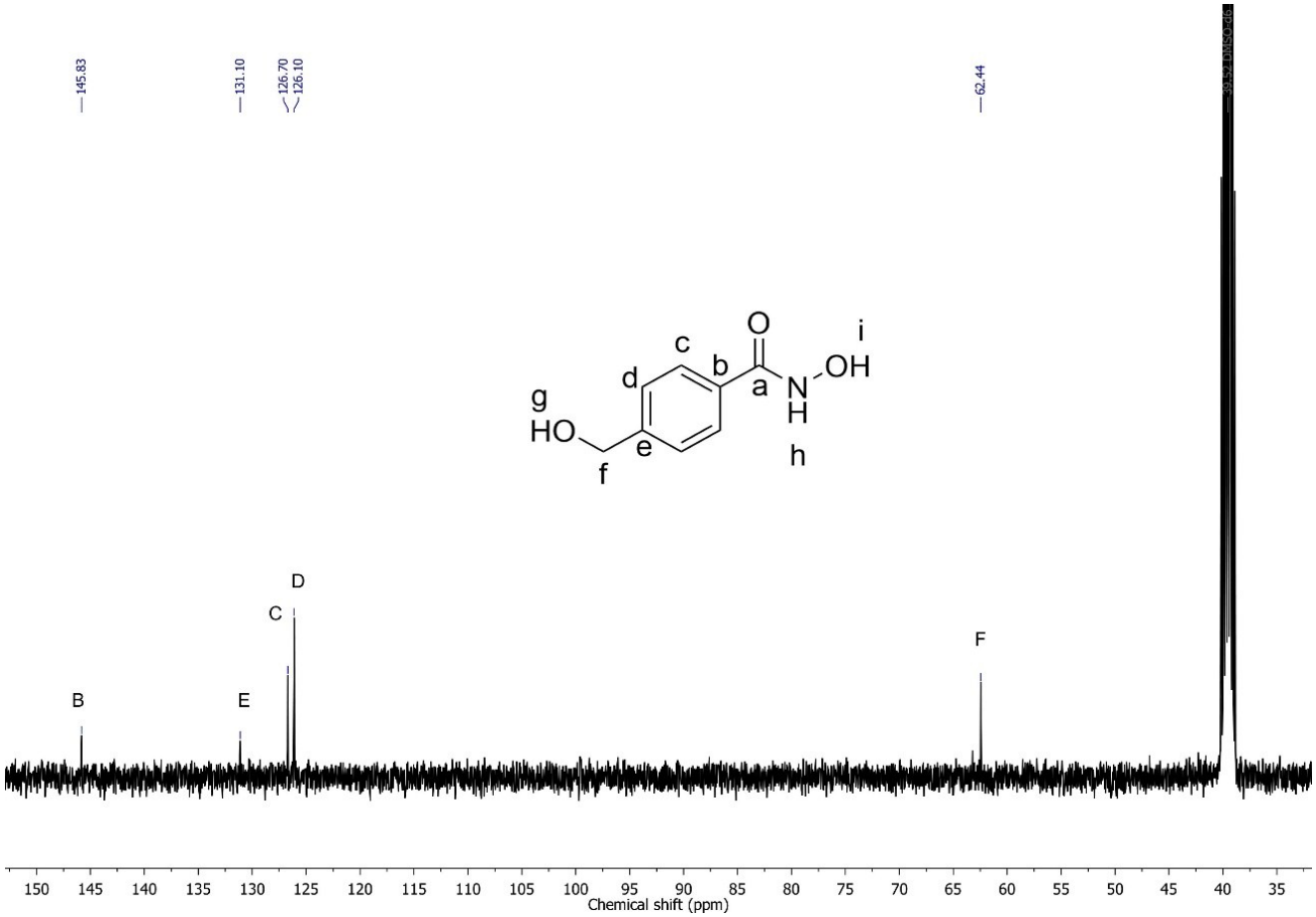

Figure S7b. ^{13}C NMR spectrum (100 MHz, DMSO-d_6) of *N*-hydroxy-4-(hydroxymethyl)benzamide **(3a).**

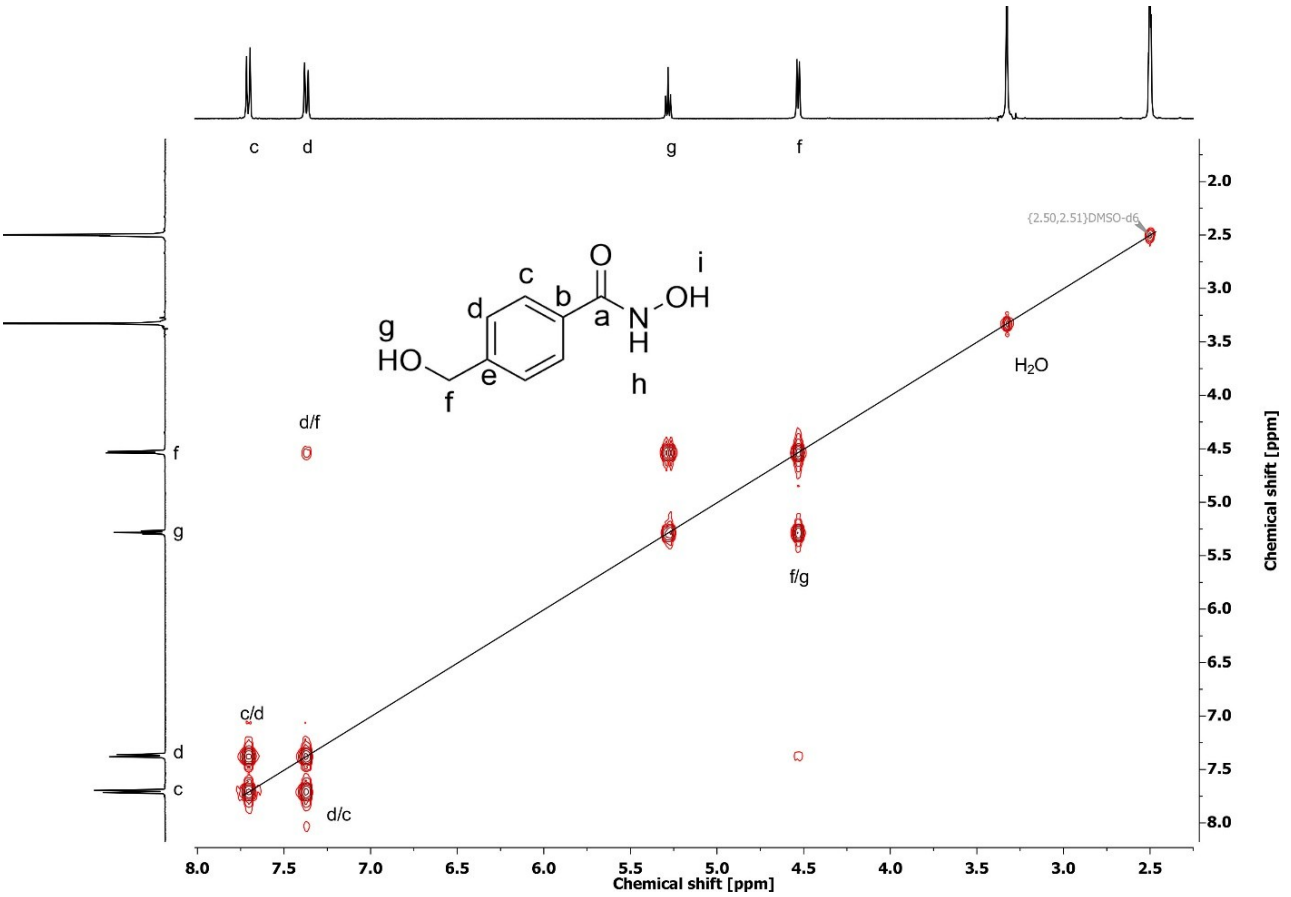

Figure S7c. ^{1}H-^{1}H COSY NMR spectrum (400 MHz, DMSO-d_6) of *N*-hydroxy-4-(hydroxymethyl)benzamide **(3a).**

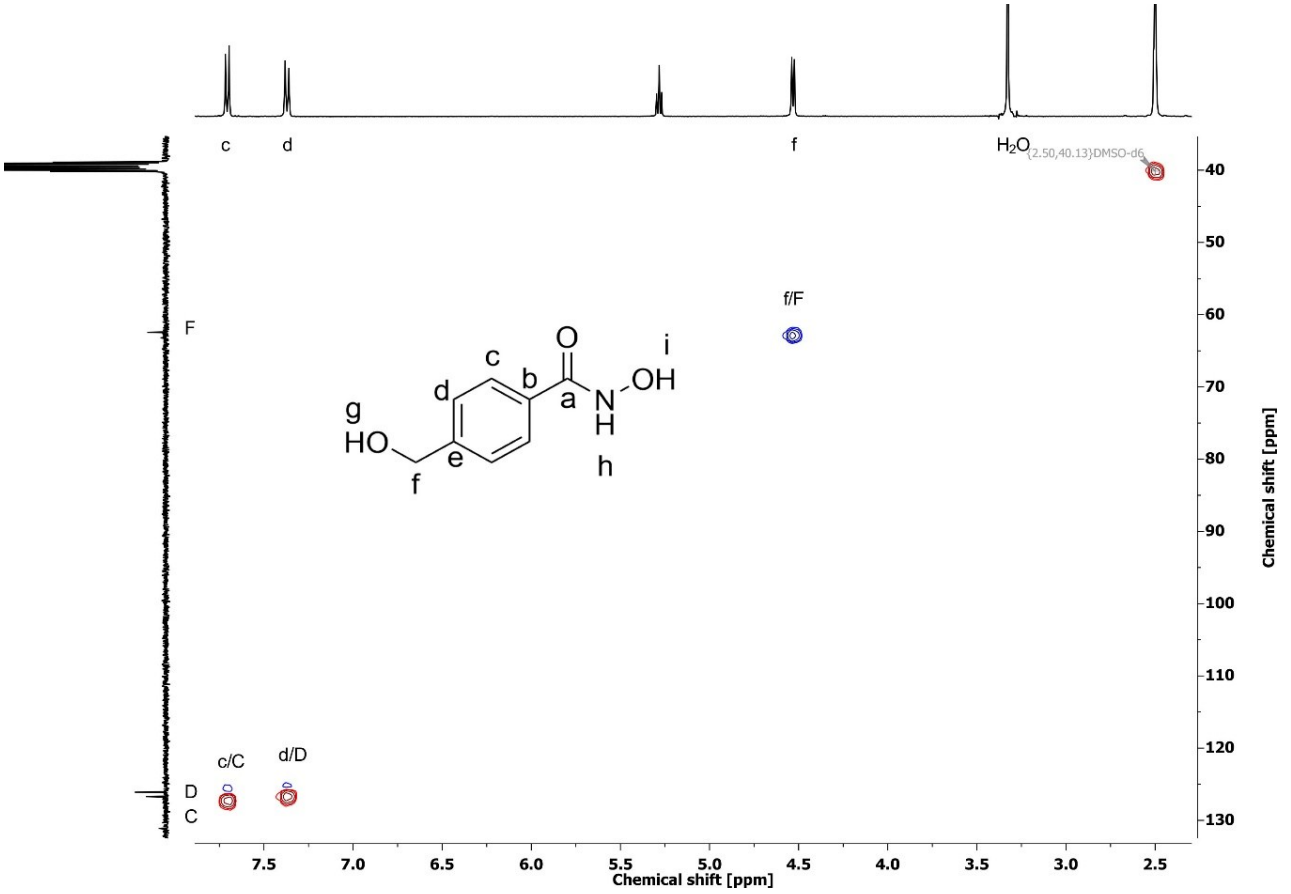

Figure S7d. ^{1}H-^{13}C HSQC NMR spectrum (400 MHz / 100 MHz, DMSO-d_6) of *N*-hydroxy-4-(hydroxymethyl)benzamide **(3a).**

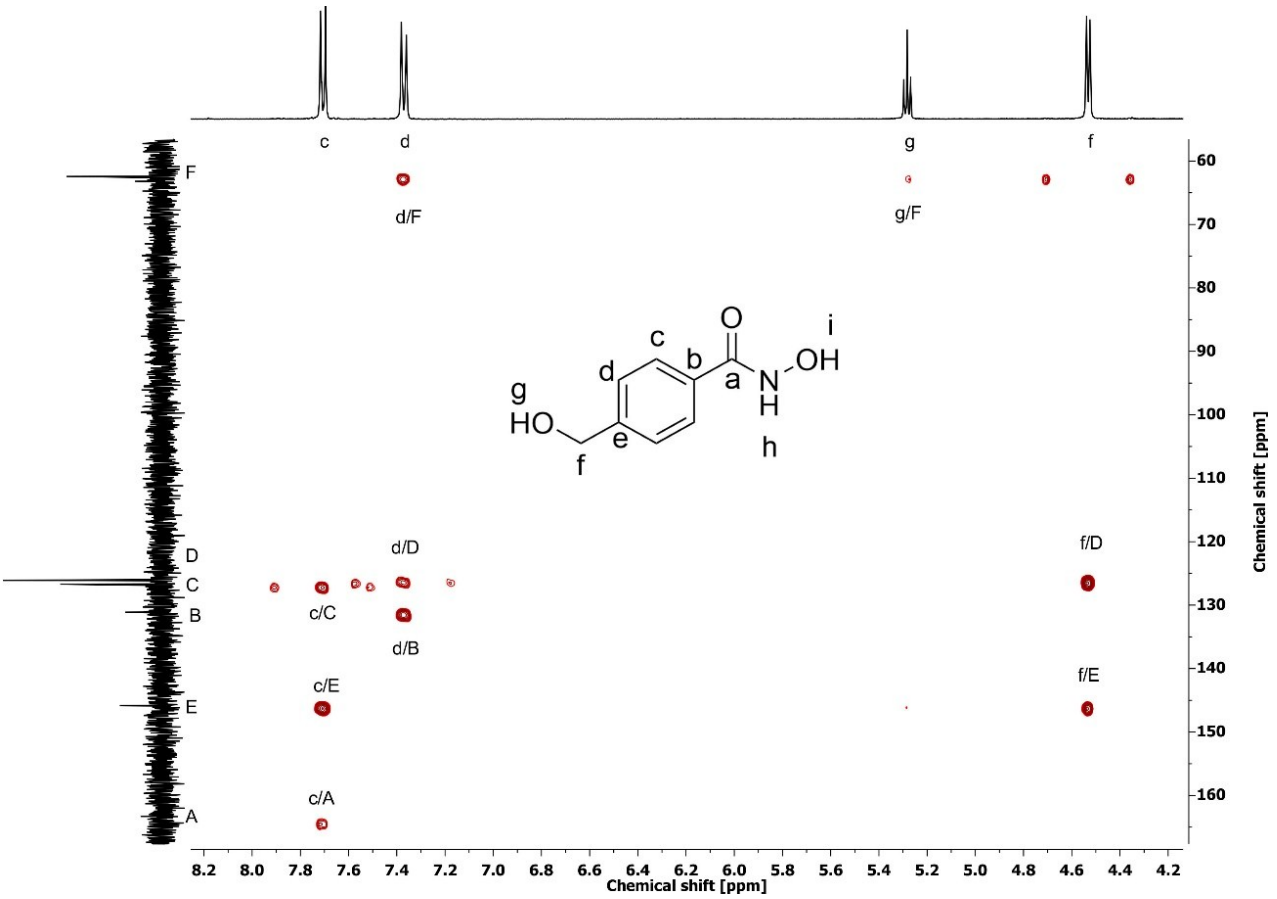

Figure S7e. ^{1}H-^{13}C HMBC NMR spectrum (400 MHz / 100 MHz, DMSO-d_6) of *N*-hydroxy-4-(hydroxymethyl)benzamide **(3a).**

Characterization of (4-(5,5-dimethyl-1,4,2-dioxazol-3-yl)phenyl)methanol (3b) ^{benzyl}HAA-OH

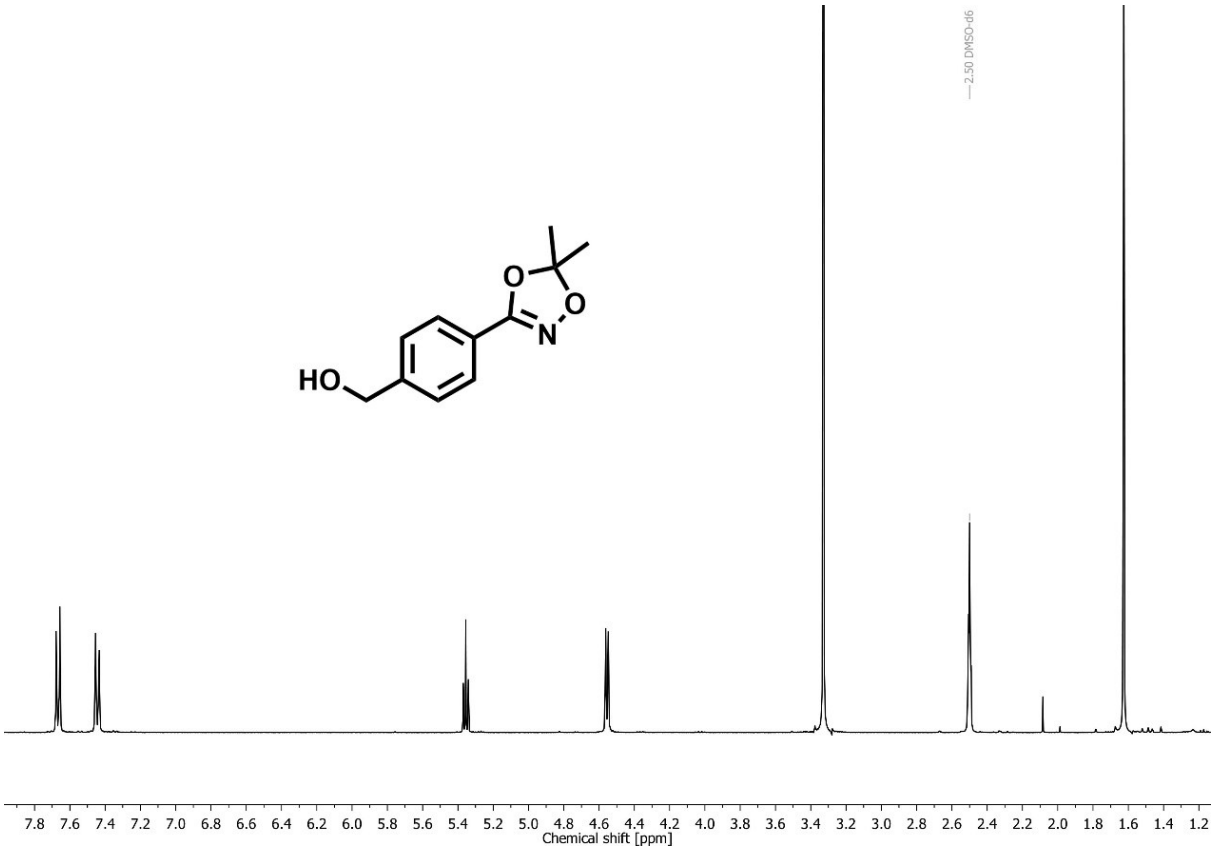

Figure S8a. ^{1}H NMR spectrum (400 MHz, DMSO-d_6) of (4-(5,5-dimethyl-1,4,2-dioxazol-3-yl)phenyl)methanol **(3b).** See synthesis procedure for detailed assignment of the signals.

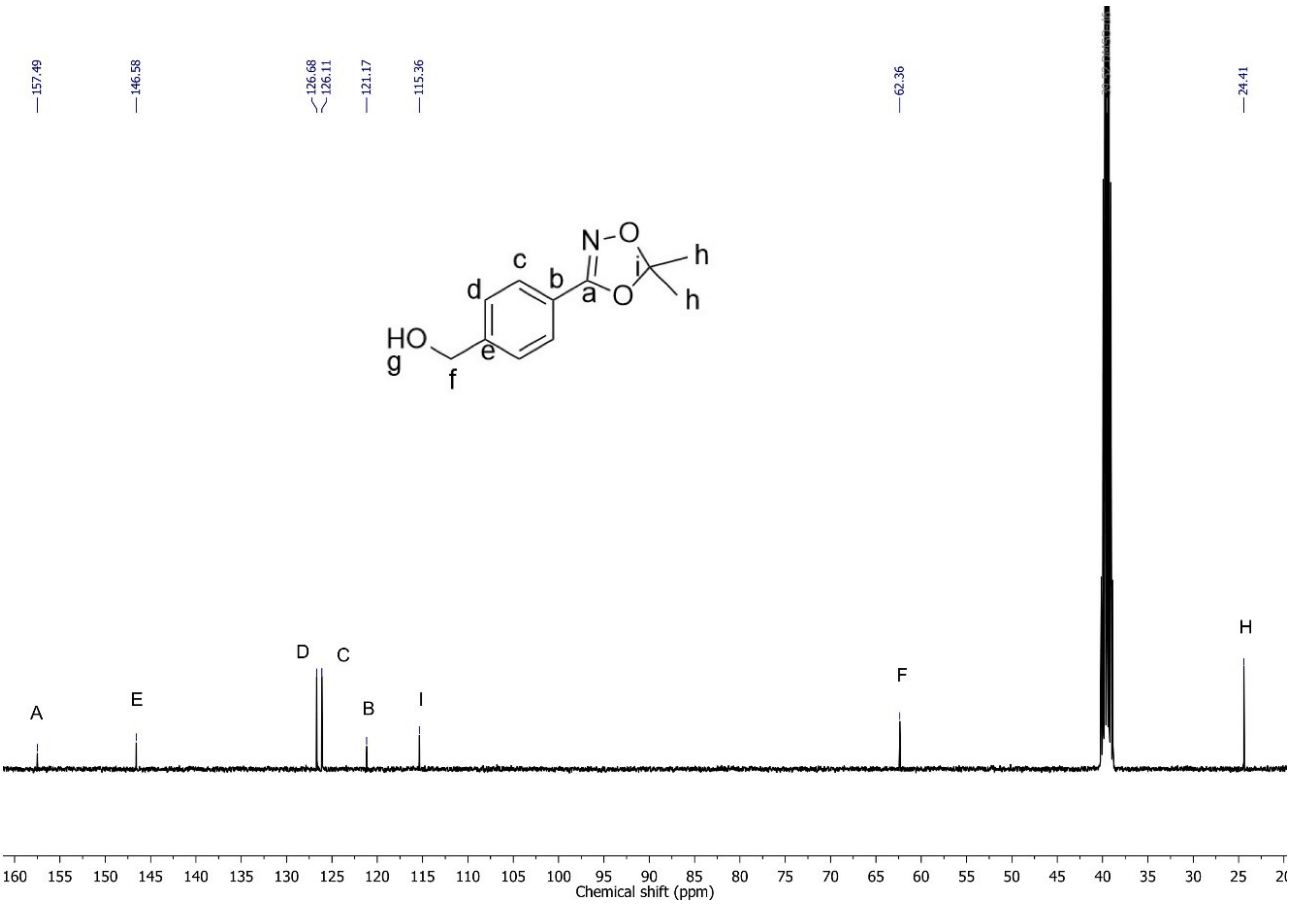

Figure S8b. ^{13}C NMR spectrum (100 MHz, DMSO-d_6) of (4-(5,5-dimethyl-1,4,2-dioxazol-3-yl)phenyl)methanol **(3b).**

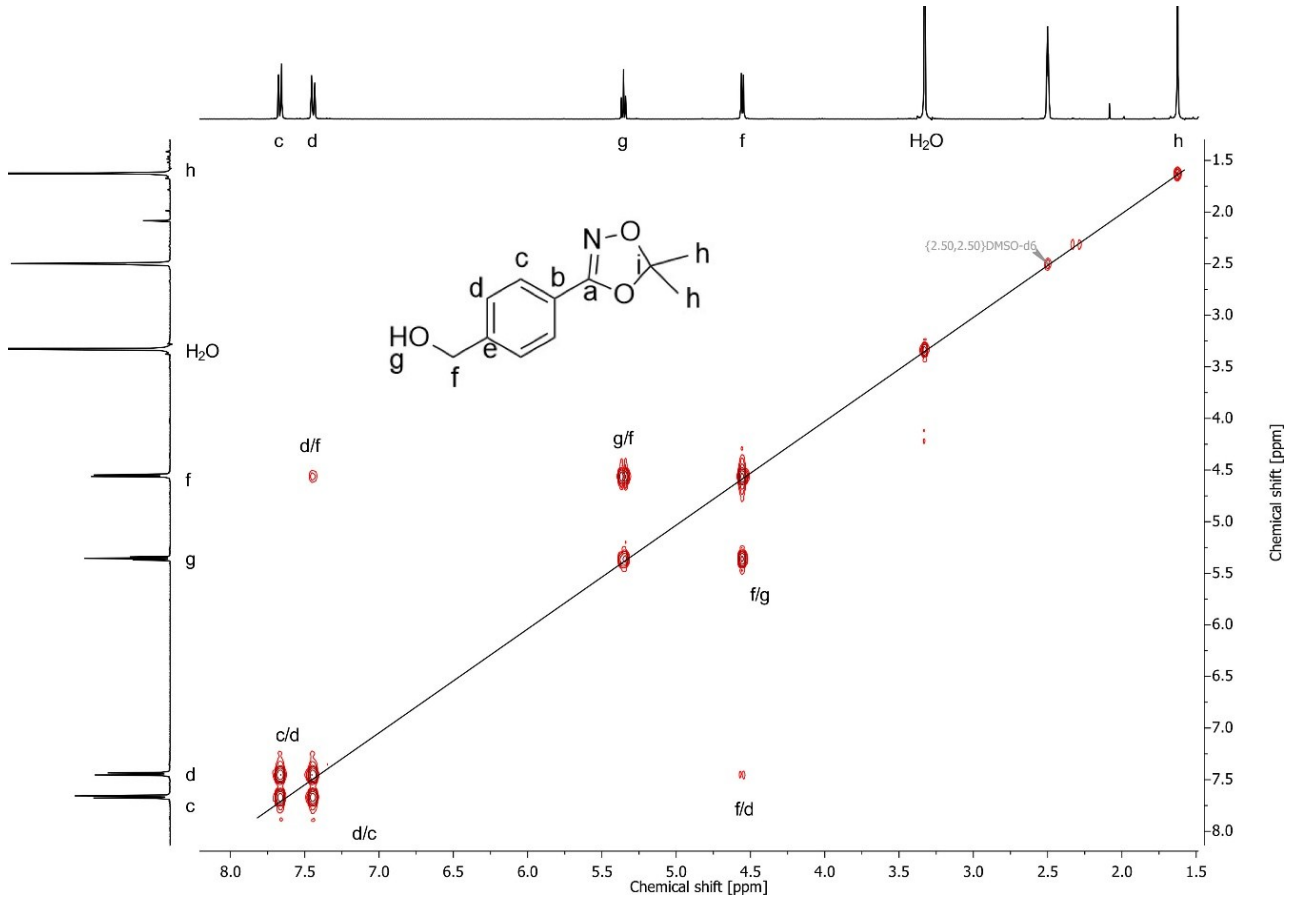

Figure S8c. ^{1}H-^{1}H COSY NMR spectrum (400 MHz, DMSO-d_6) of (4-(5,5-dimethyl-1,4,2-dioxazol-3-yl)phenyl)methanol **(3b).**

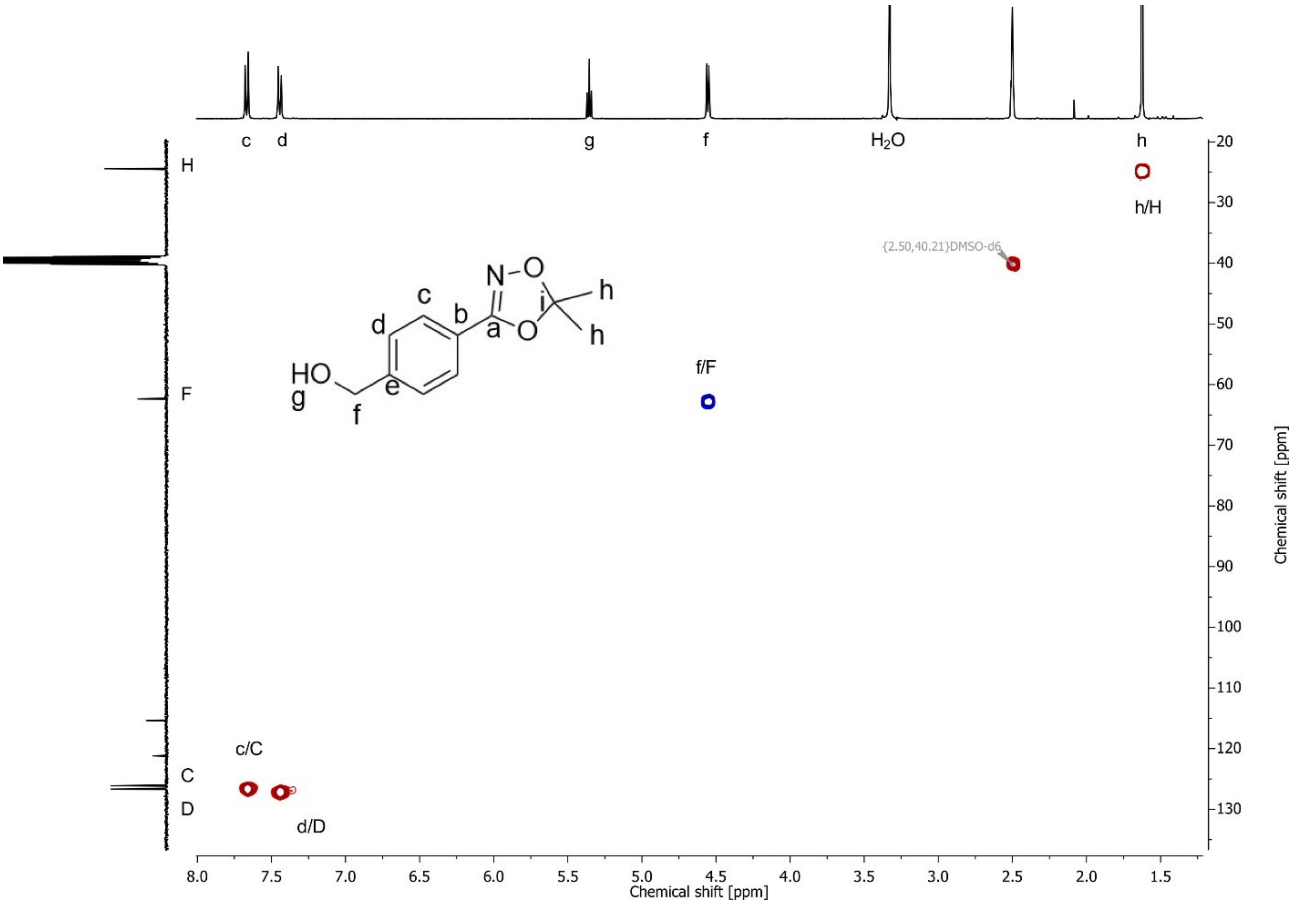

Figure S8d. ^{1}H-^{13}C HSQC NMR spectrum (400 MHz / 100 MHz, DMSO-d_6) of (4-(5,5-dimethyl-1,4,2-dioxazol-3-yl)phenyl)methanol **(3b).**

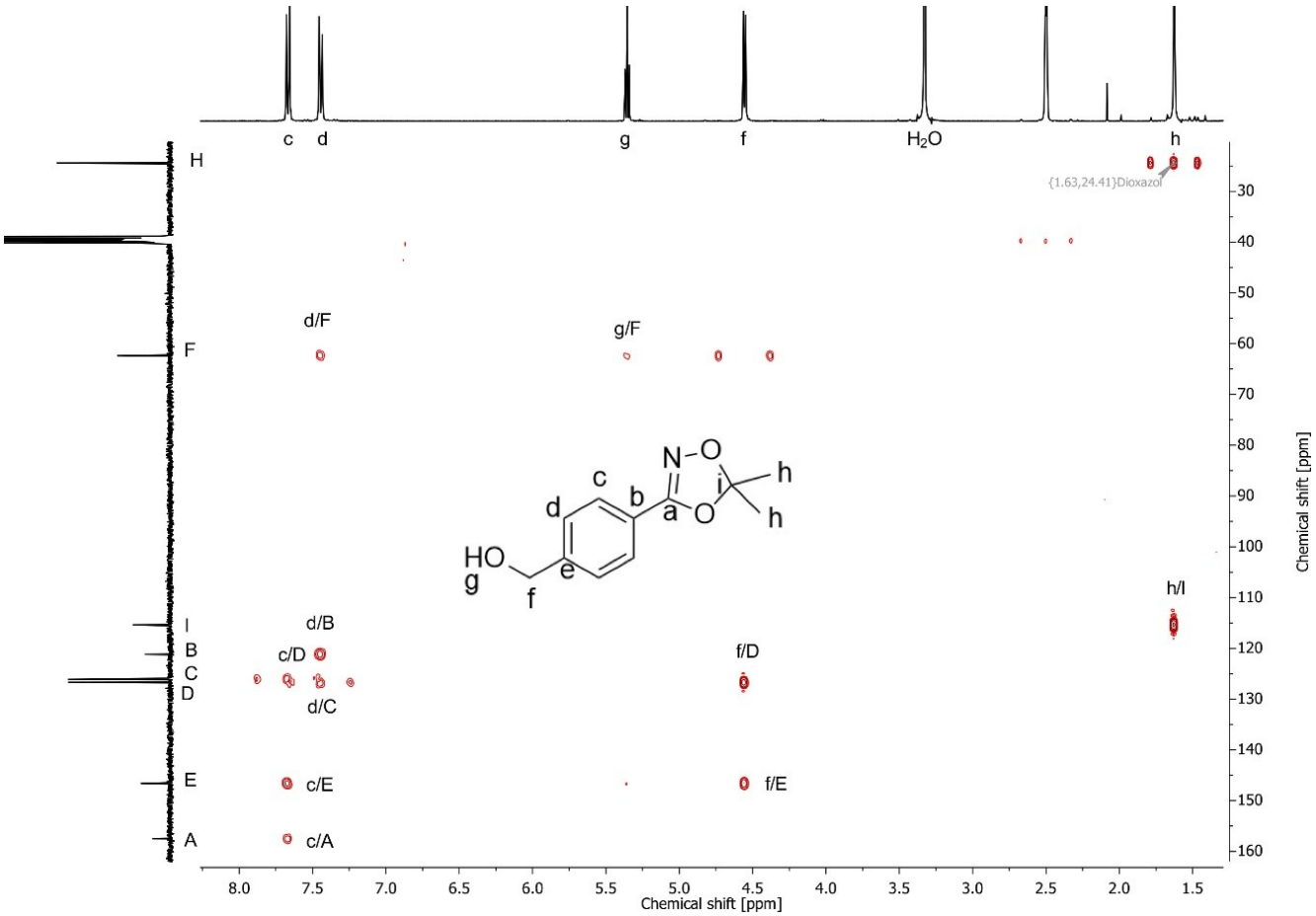

Figure S8e. ^{1}H-^{13}C HMBC NMR spectrum (400 MHz / 100 MHz, DMSO-d_6) of (4-(5,5-dimethyl-1,4,2-dioxazol-3-yl)phenyl)methanol **(3b).**

Characterization of *N*,6-dihydroxyhexanamide (4a)

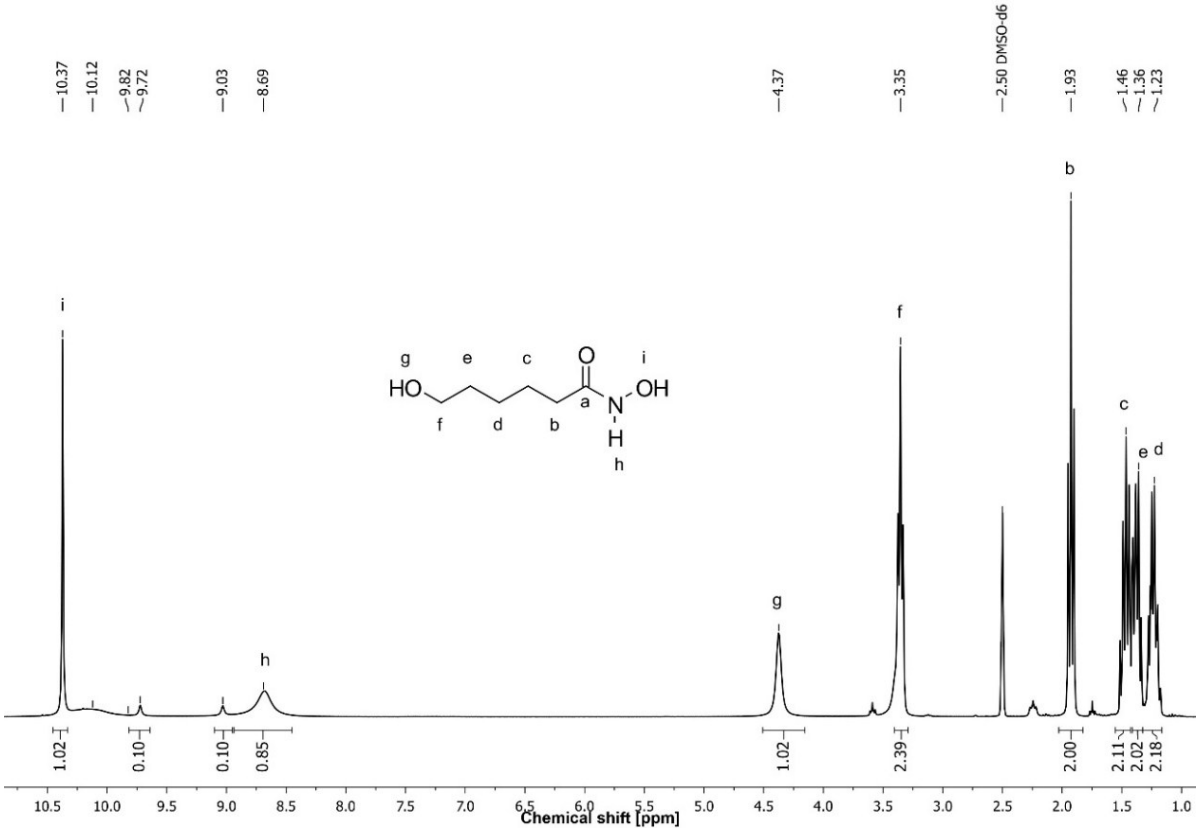

Figure S9a. ^{1}H NMR spectrum (300 MHz, DMSO-d_6) of *N*,6-dihydroxyhexanamide **(4a).**

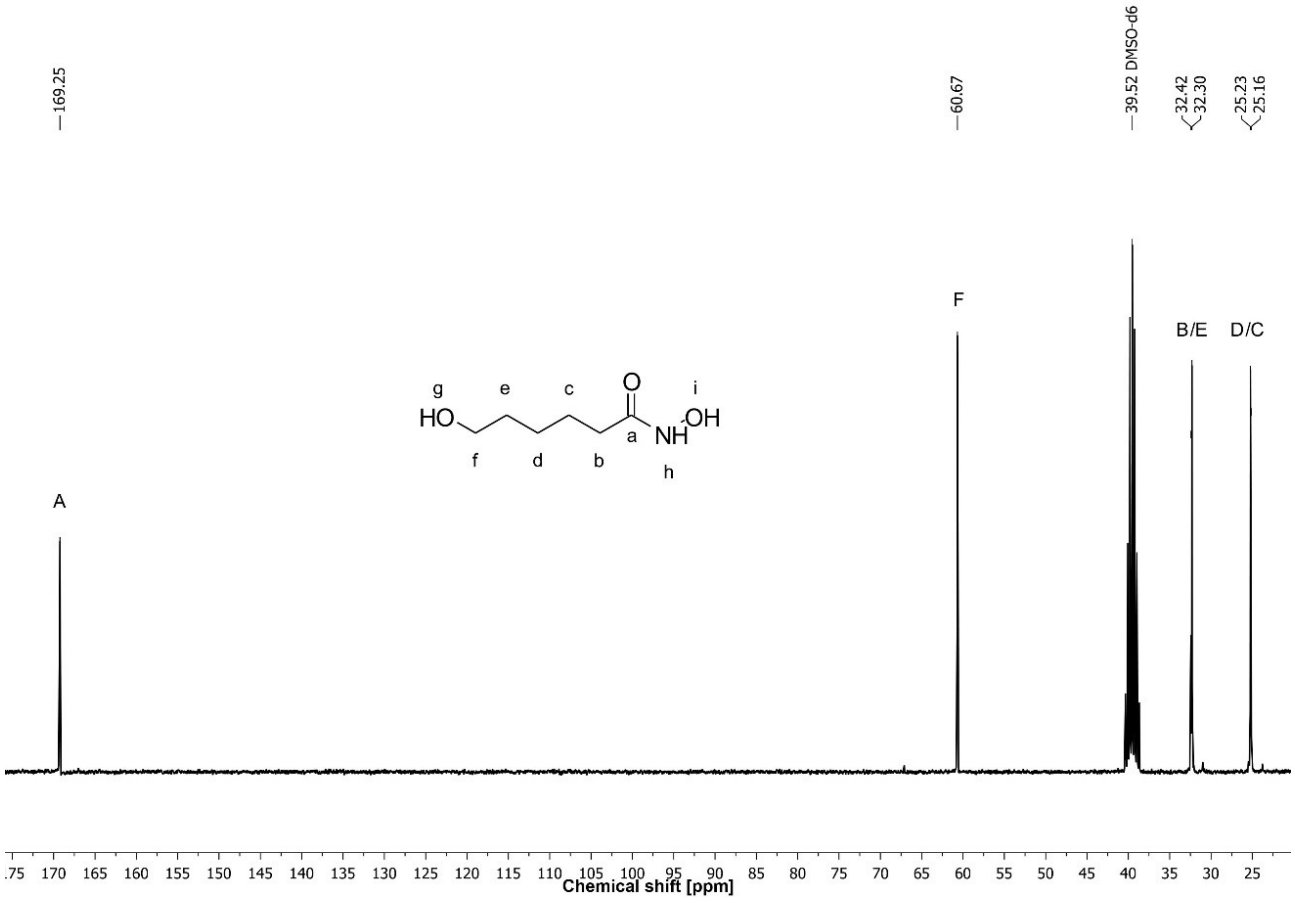

Figure S9b. ^{13}C NMR spectrum (75 MHz, DMSO-d_6) of *N*,6-dihydroxyhexanamide **(4a).**

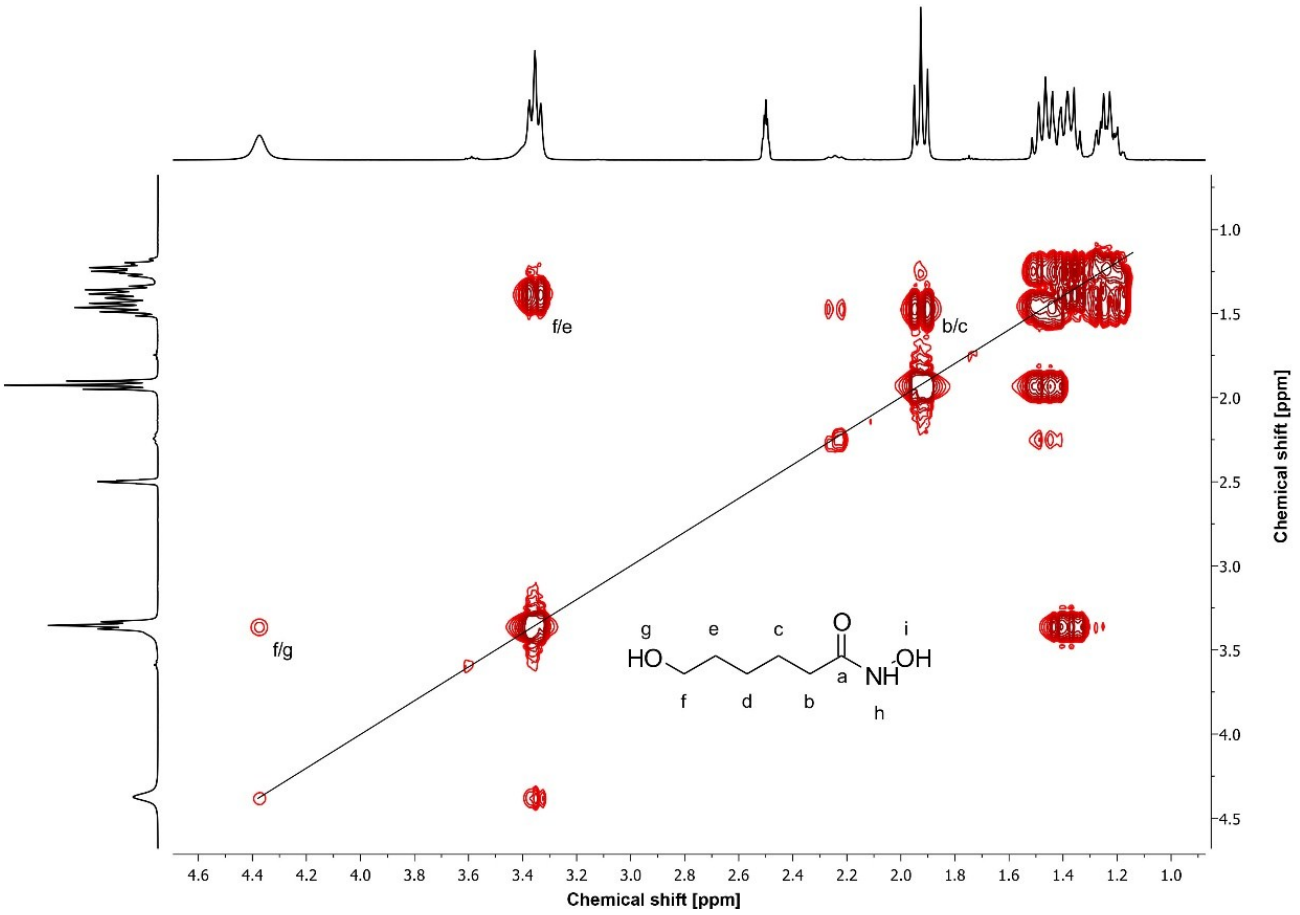

Figure S9c. ^{1}H-^{1}H COSY NMR spectrum (300 MHz, DMSO-d_6) of *N*,6-dihydroxyhexanamide **(4a).**

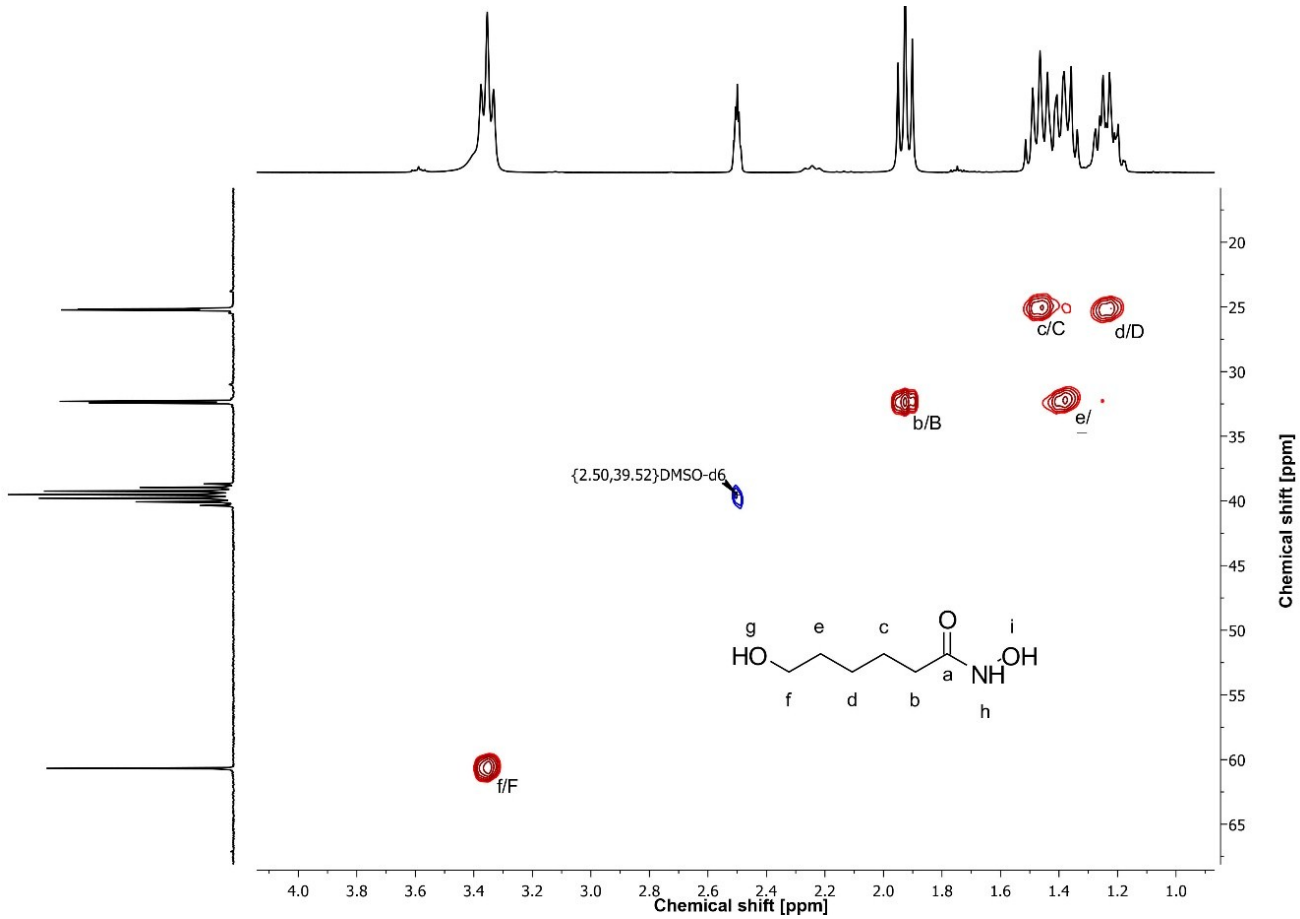

Figure S9d. ^{1}H-^{13}C HSQC NMR spectrum (300 MHz / 100 MHz, DMSO-d_6) of *N*,6-dihydroxyhexanamide **(4a).**

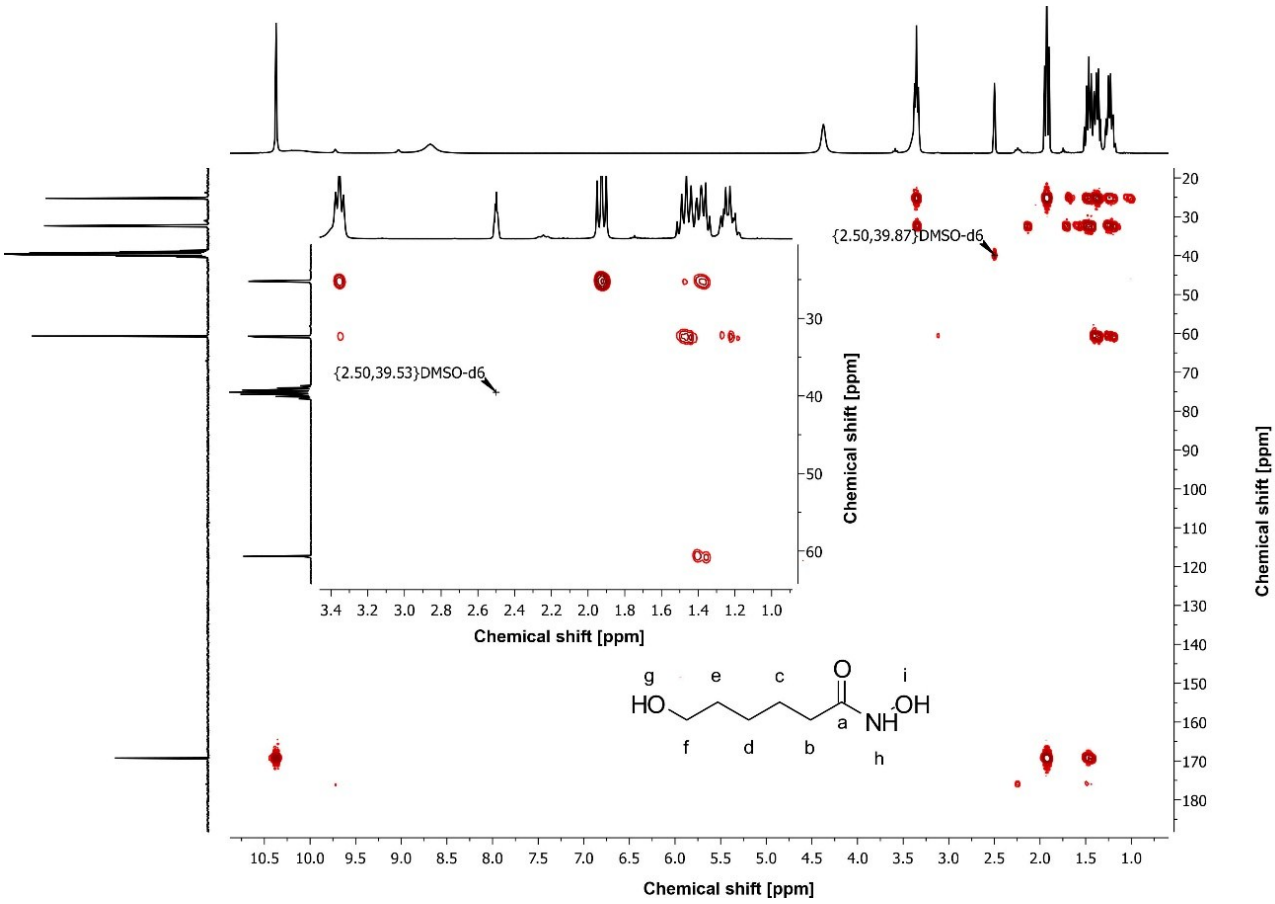

Figure S9e. ^{1}H-^{13}C HMBC NMR spectrum (300 MHz / 100 MHz, DMSO-d_6) of *N*,6-dihydroxyhexanamide **(4a).**

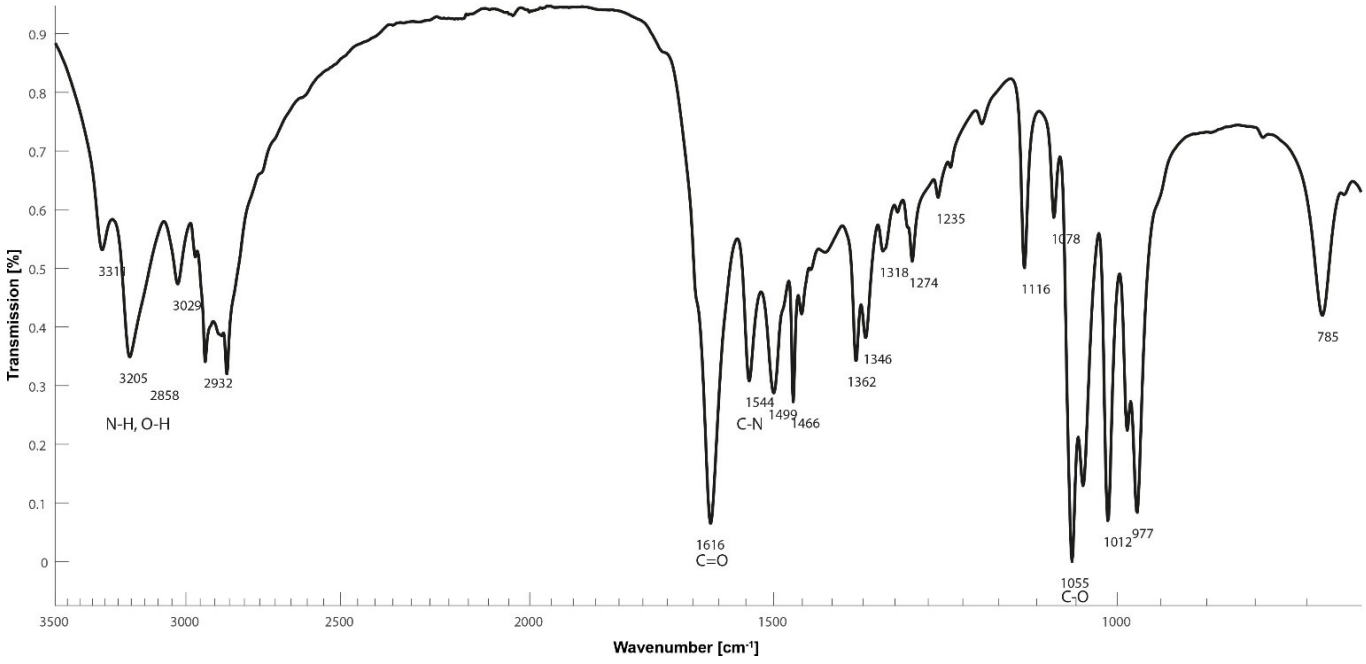

Figure S9f. FT-ATR-IR spectrum of *N*,6-dihydroxyhexanamide **(4a).**

Characterization of 5-(5,5-dimethyl-1,4,2-dioxazol-3-yl)pentan-1-ol (4b)

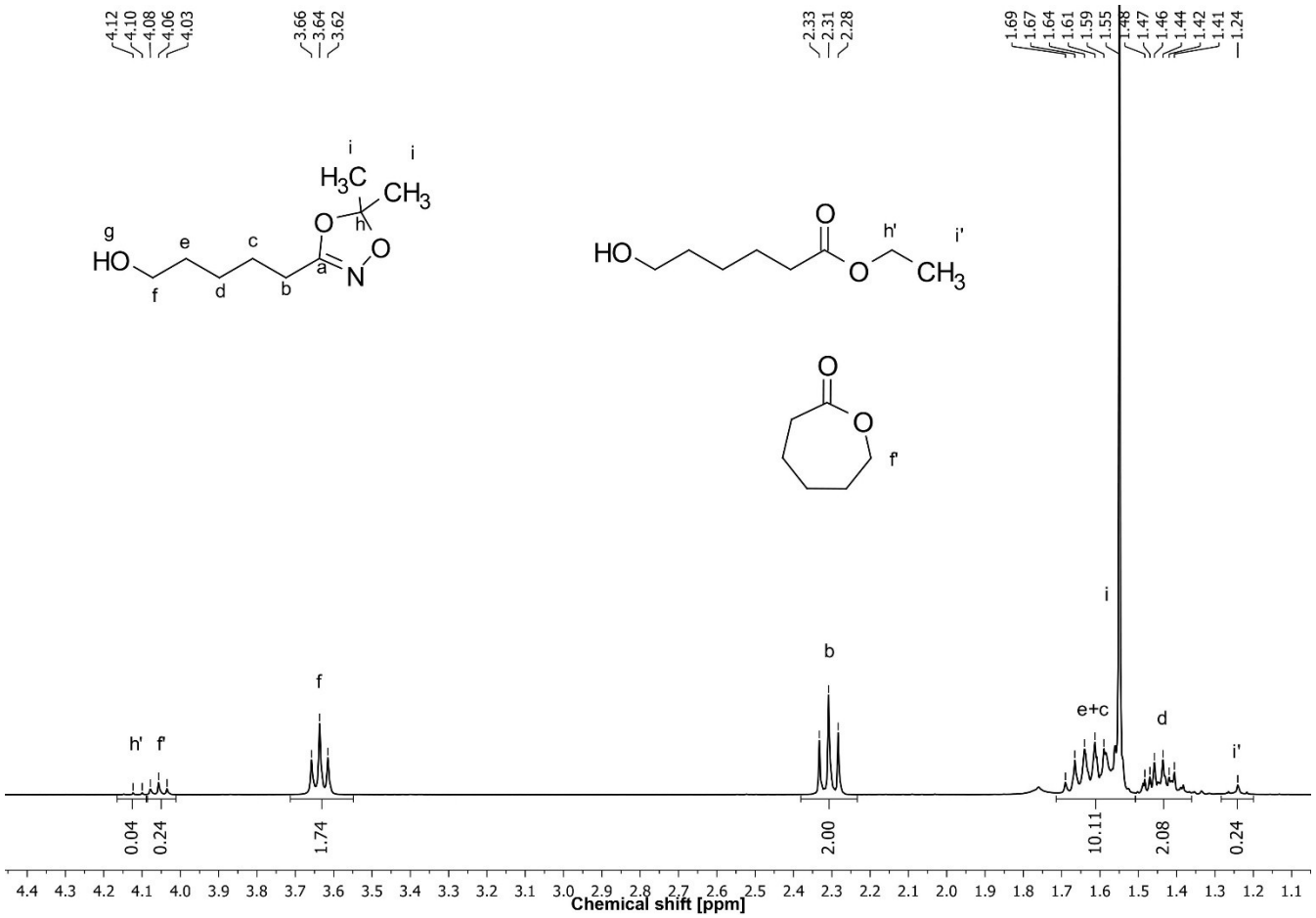

Figure S10. ^{1}H NMR spectrum (300 MHz, DMSO-d_6) of 5-(5,5-dimethyl-1,4,2-dioxazol-3-yl)pentan-1-ol **(4b).** The caprolactone signals originate from the side reaction during transketalization reaction.

Characterization of 5,5-dimethyl-3-(4-(2-(oxiran-2-ylmethoxy)ethoxy)phenyl) -1,4,2-dioxazole (1d)

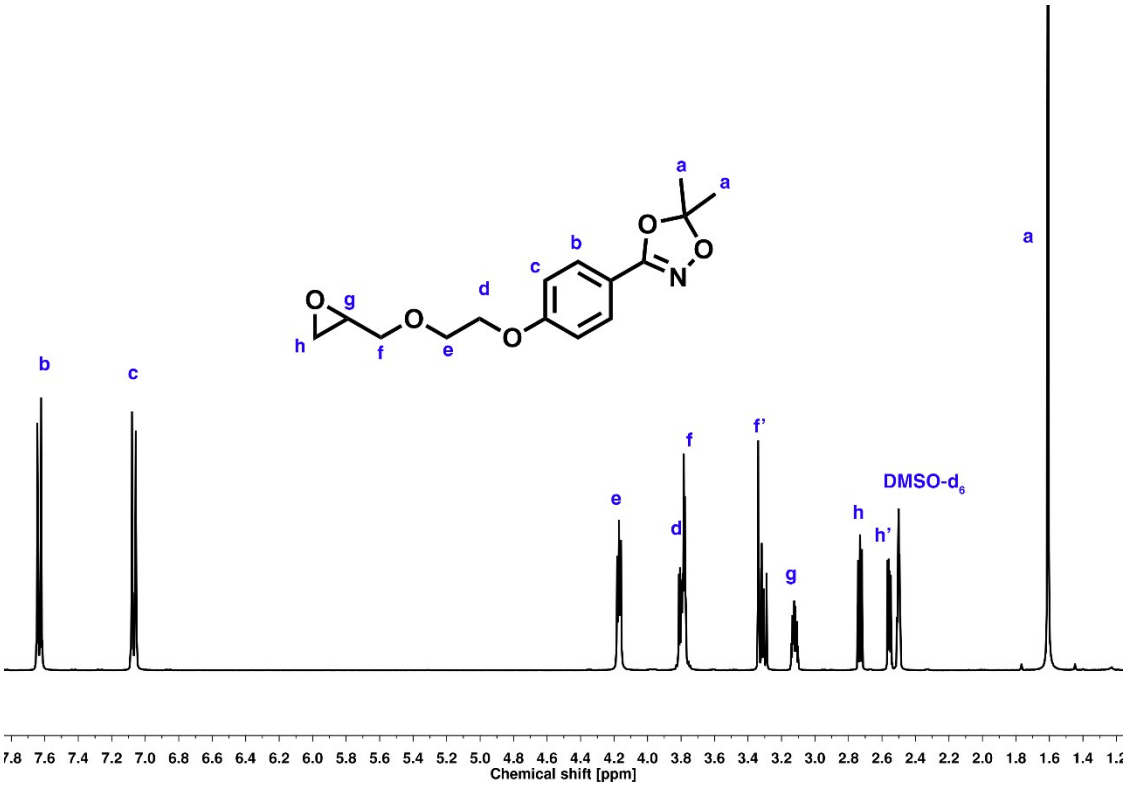

Figure S11. ^{1}H NMR spectrum (400 MHz, DMSO-d_6) of 5,5-dimethyl-3-(4-(2-(oxiran-2-ylmethoxy)ethoxy)phenyl) -1,4,2-dioxazole **(1d)**

Characterization of 2-(4-(5,5-dimethyl-1,4,2-dioxazol-3-yl)phenoxy)ethyl methacrylate (1e)

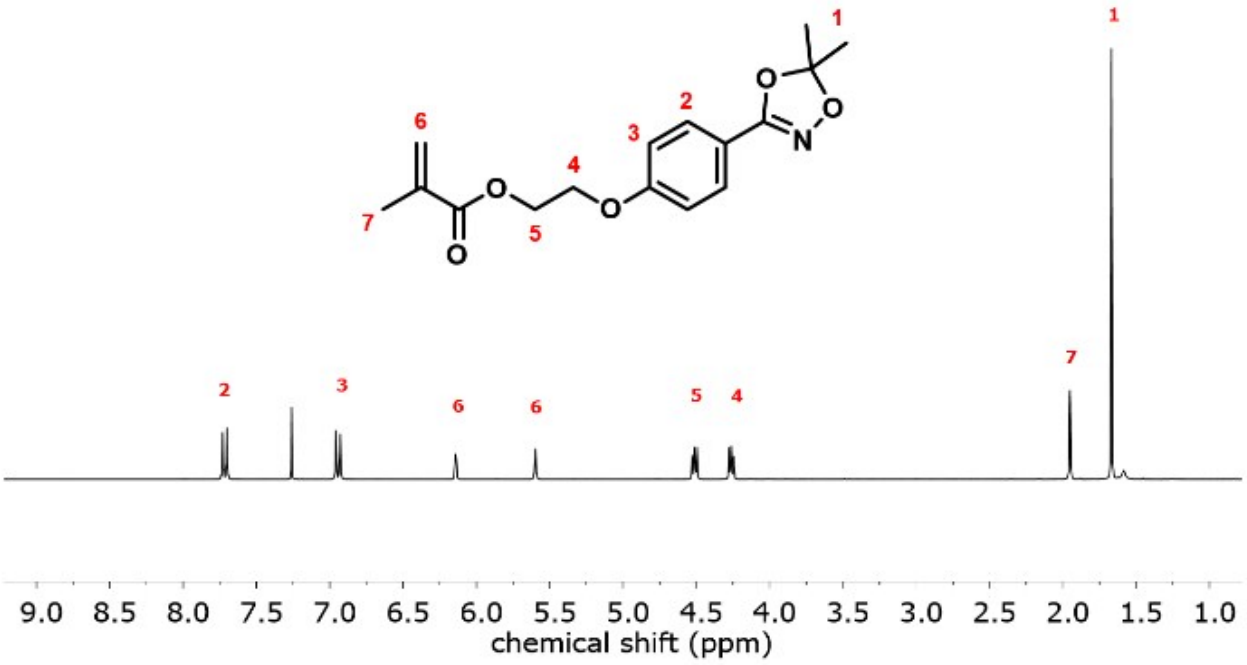

Figure S12. ^{1}H NMR spectrum (300 MHz, DMSO-d_6) of 2-(4-(5,5-dimethyl-1,4,2-dioxazol-3-yl)phenoxy)ethyl methacrylate **(1e).**

Characterization of HAA-PEG (P1a), HA-PEG (P1b) and ^{benzyl}HAA-PEG (P2a) polymers

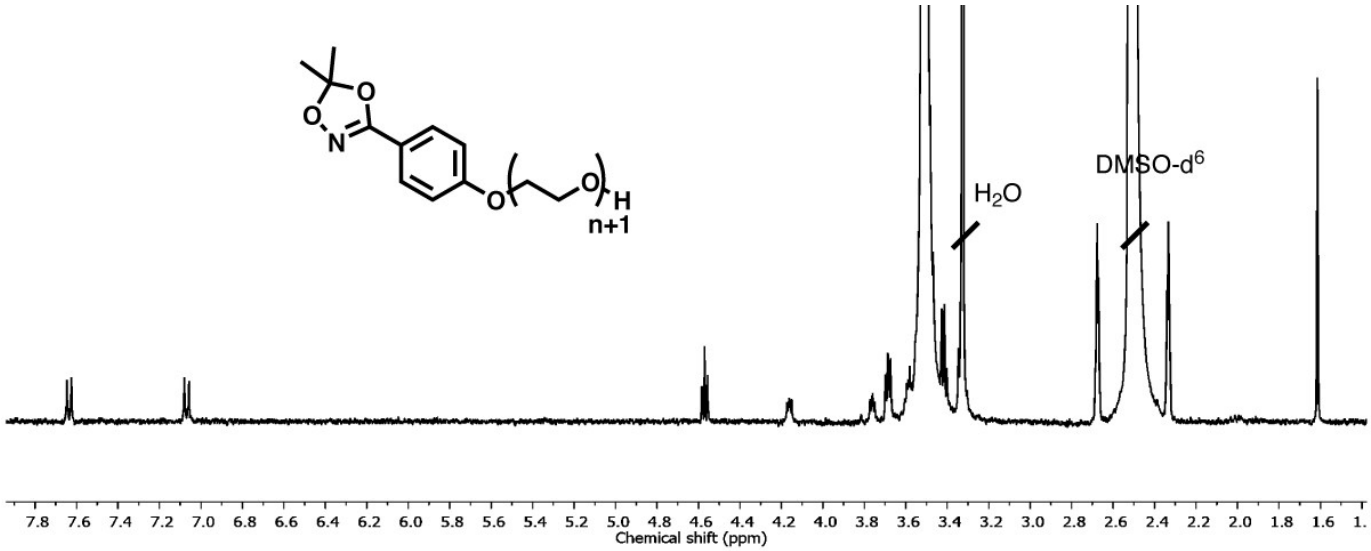

Figure S13a. Exemplary ^{1}H NMR spectrum (400 MHz, DMSO-d_6) of HAA-PEG (**P1a**). See synthesis procedure for detailed assignment of the signals.

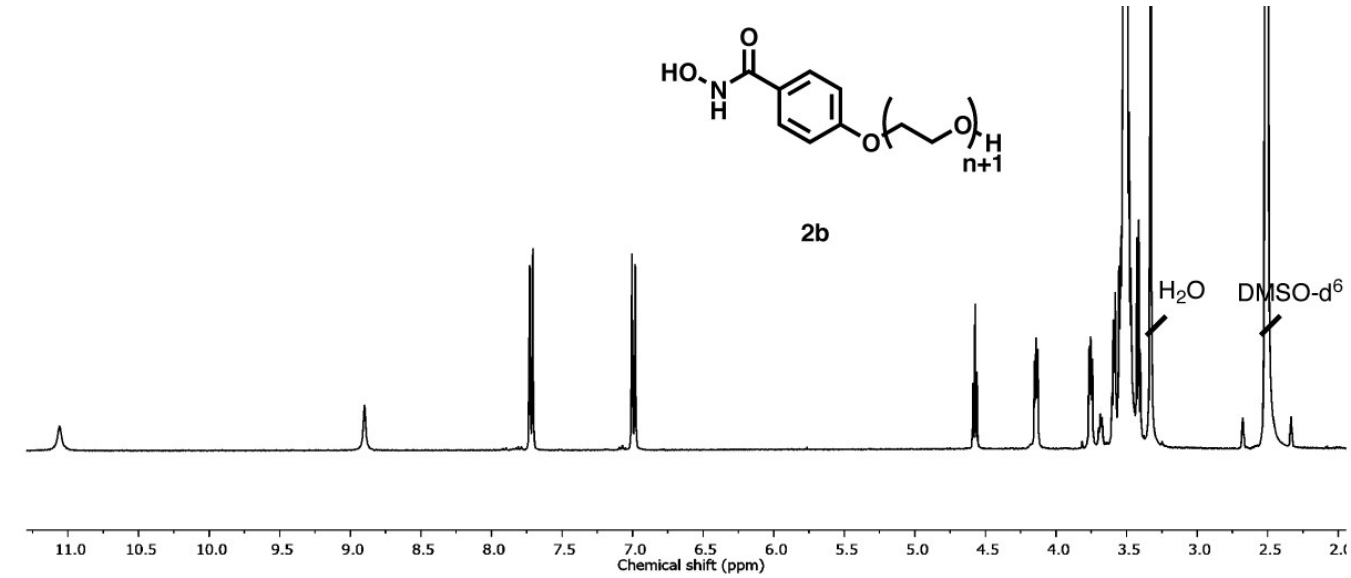

Figure S13b. Exemplary ^{1}H NMR spectrum (400 MHz, DMSO-d_6) of HA-PEG (**P1b**). See synthesis procedure for detailed assignment of the signals.

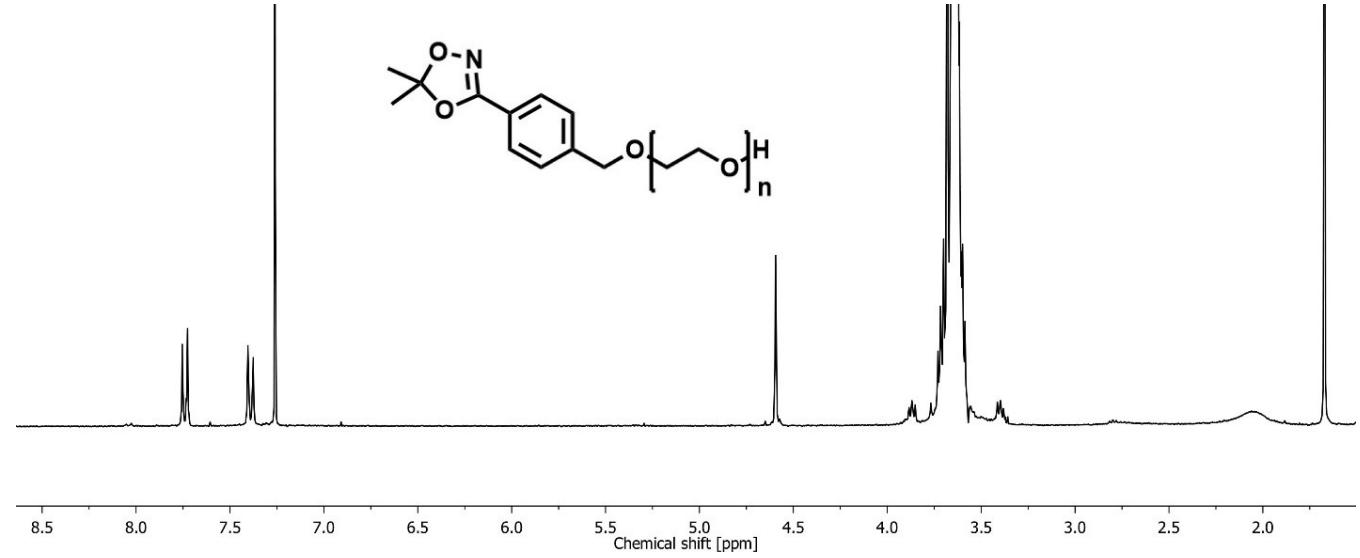

Figure S14. Exemplary ^{1}H NMR spectrum (300 MHz, $CDCl_3$) of ^{benzyl}HAA-PEG (**P2a**).

Characterization of HAA-PPO (P3a), ^{benzyl}HAA-PPO (P4a), HAA-PEEGE (P5a) and ^{benzyl}HAA-PEEGE (P6a) polymers

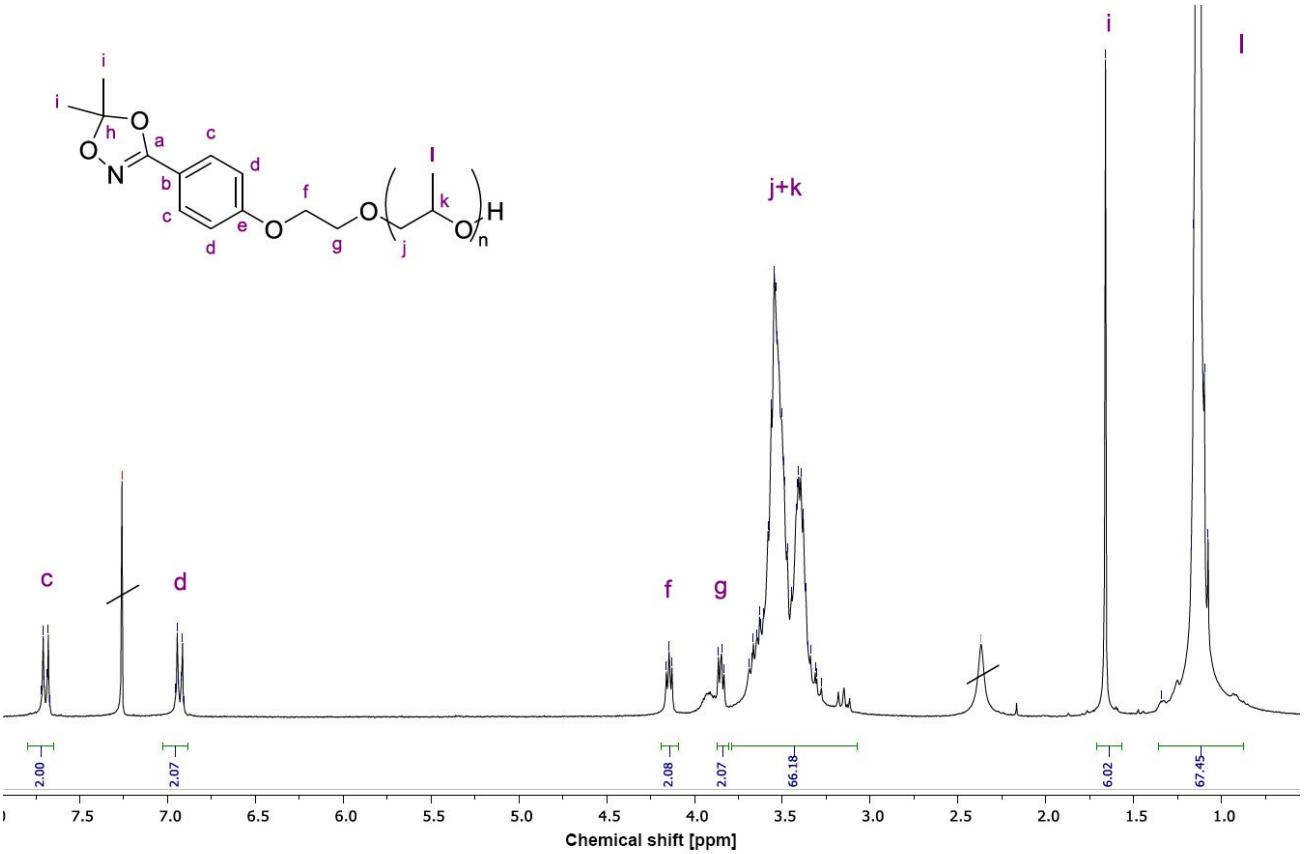

Figure S15. Exemplary ^{1}H NMR spectrum (300 MHz, $CDCl_3$) of HAA-PPO (**P3a**).

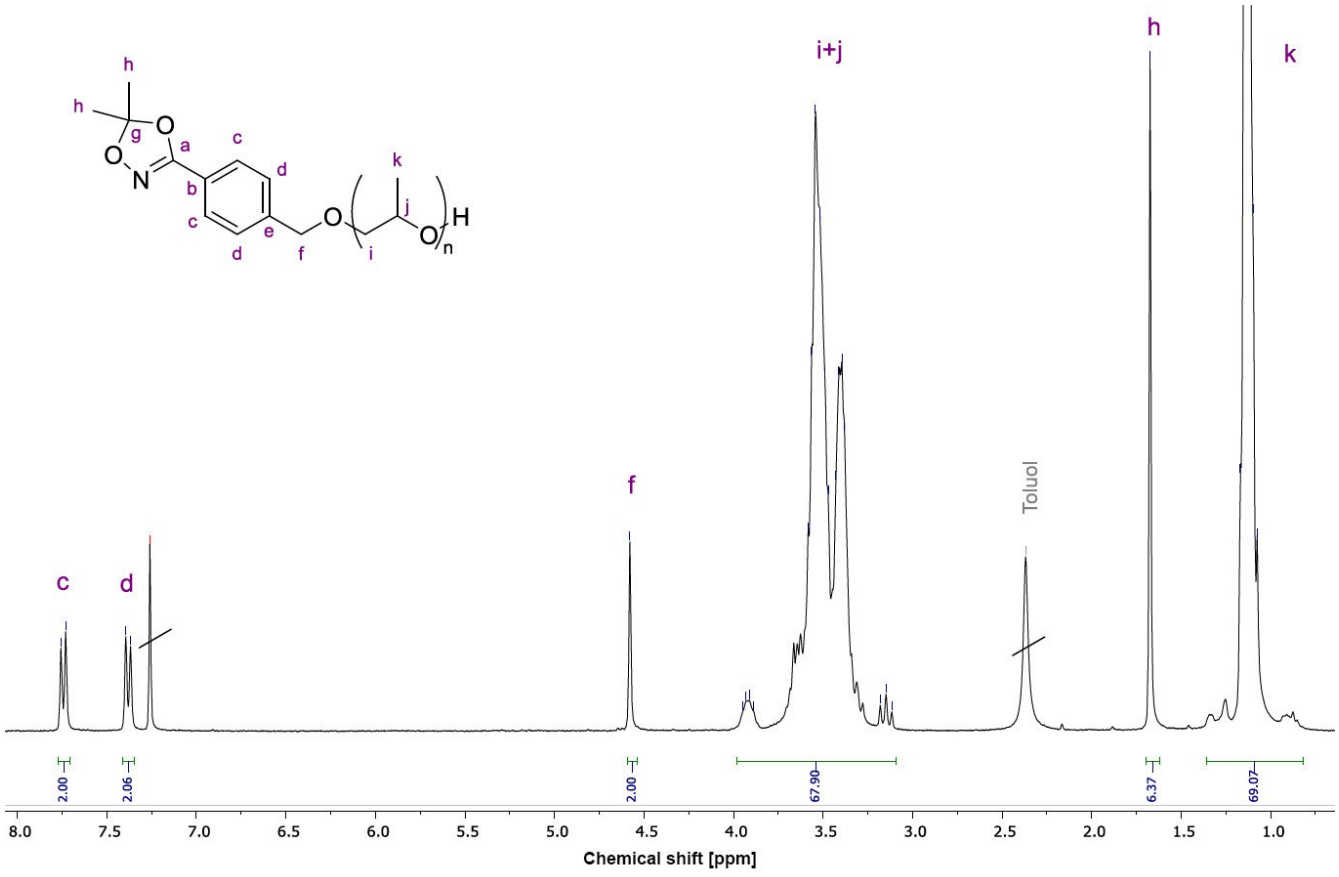

Figure S16. Exemplary ^{1}H NMR spectrum (300 MHz, $CDCl_3$) of ^{benzyl}HAA-PPO (**P4a**).

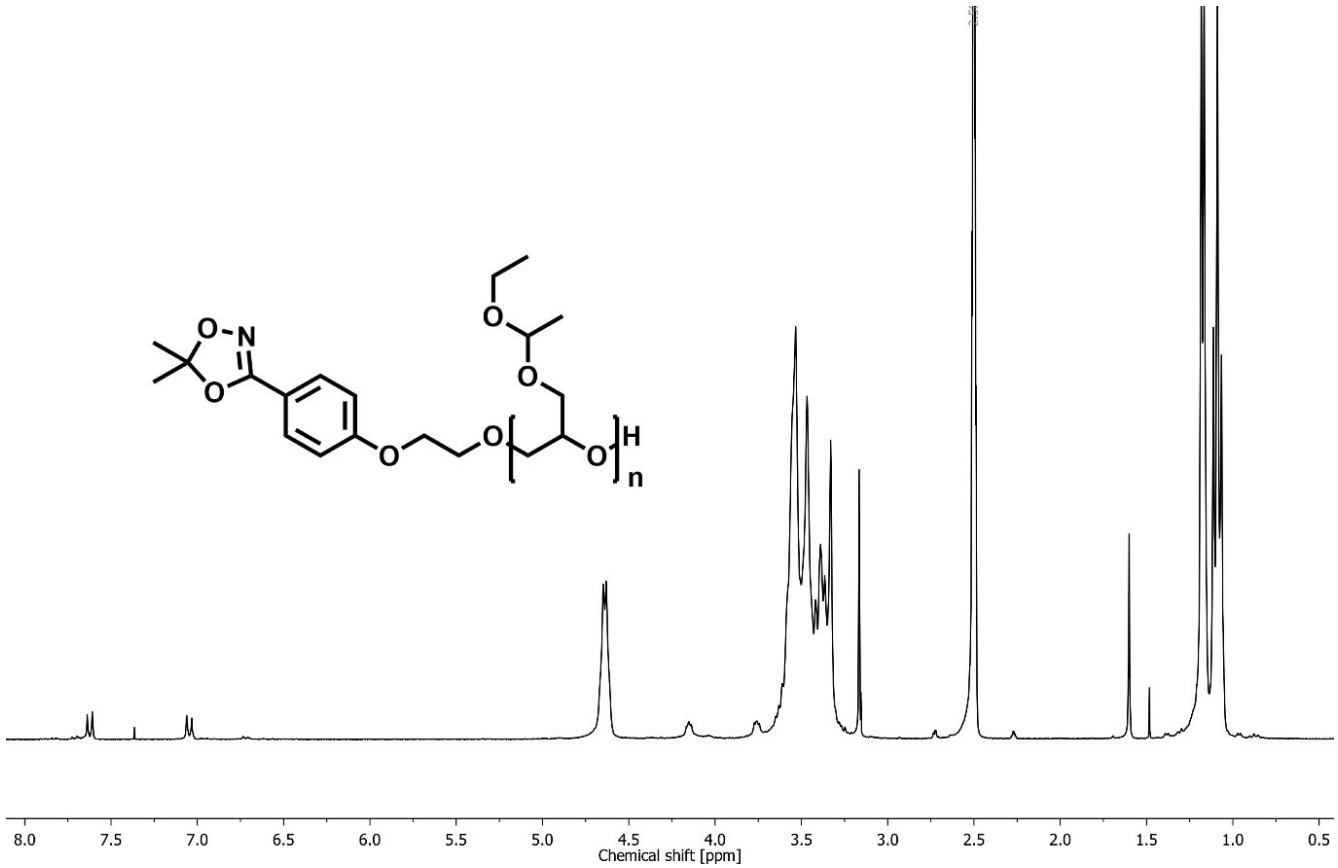

Figure S17. Exemplary ^{1}H NMR spectrum (300 MHz, $CDCl_3$) of HAA-PEEGE (**P5a**).

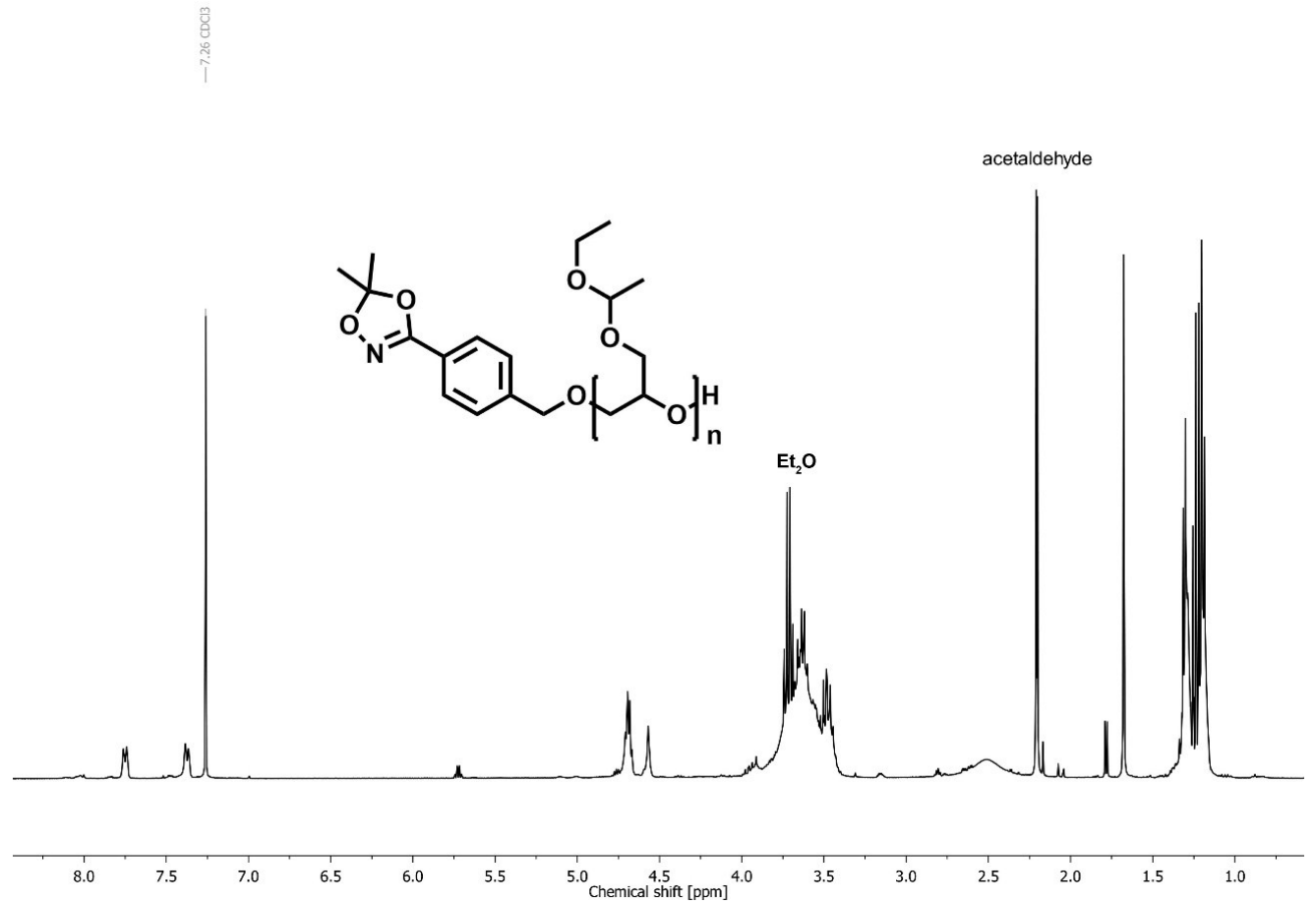

Figure S18. Exemplary ^{1}H NMR spectrum (300 MHz, $CDCl_3$) of ^{benzyl}HAA-PEEGE (**P6a**).

Polymer mass spectroscopy characterization

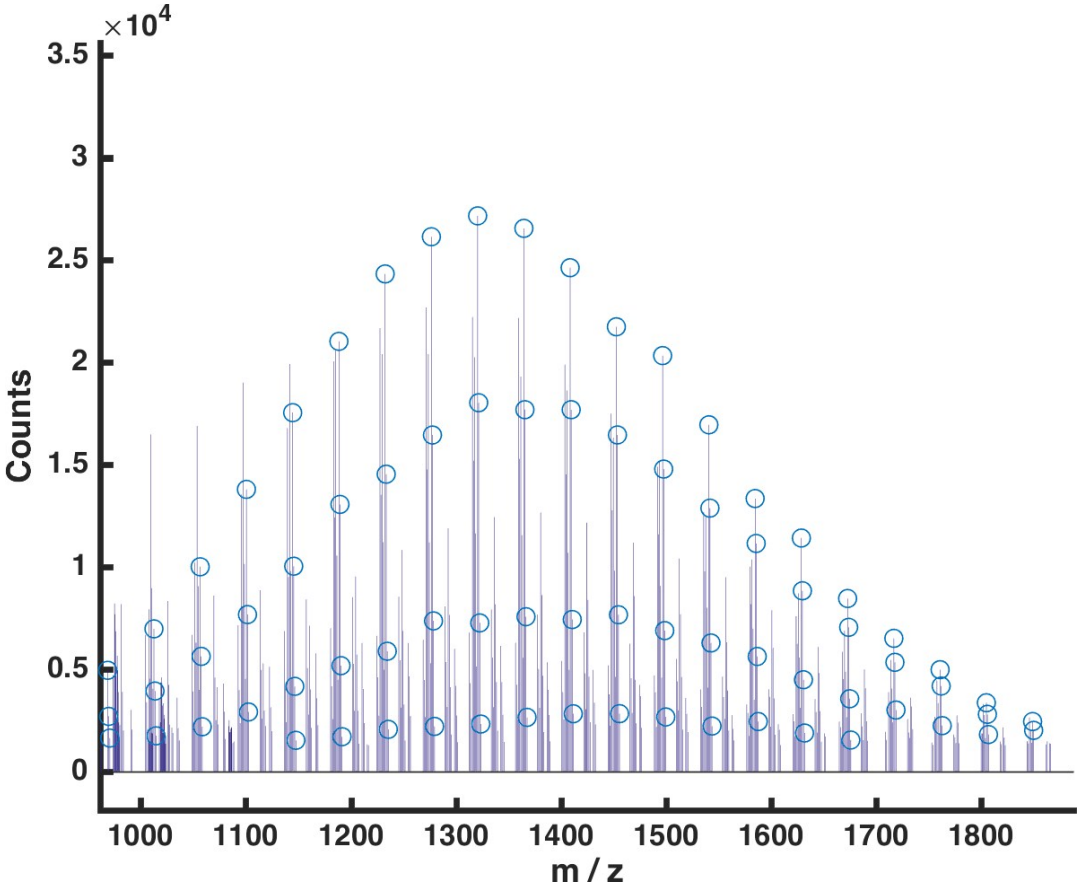

Figure S19. ESI-MS spectrum of HAA-PEG$_{31}$. The circles denote the HAA-PEG distribution with sodium as a counter ion.

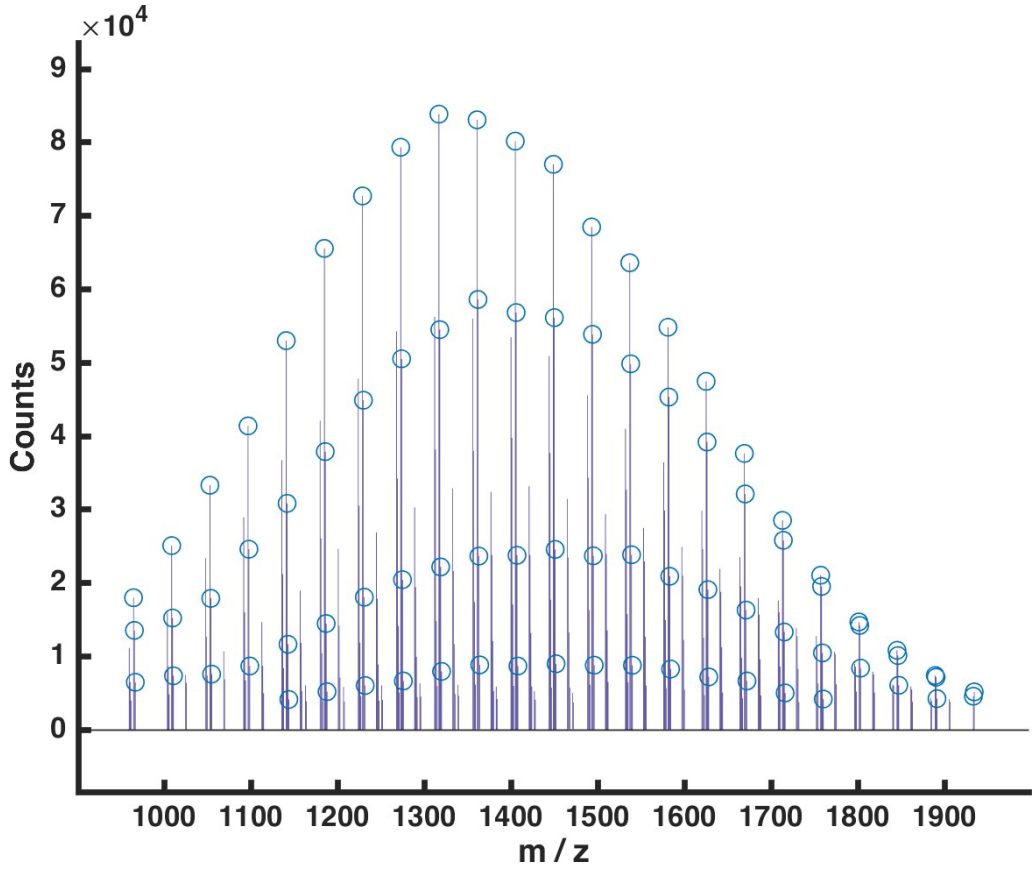

Figure S20. ESI-MS spectrum of HA-PEG$_{31}$. The circles denote the HA-PEG distribution with sodium as a counter ion.

Complexation properties

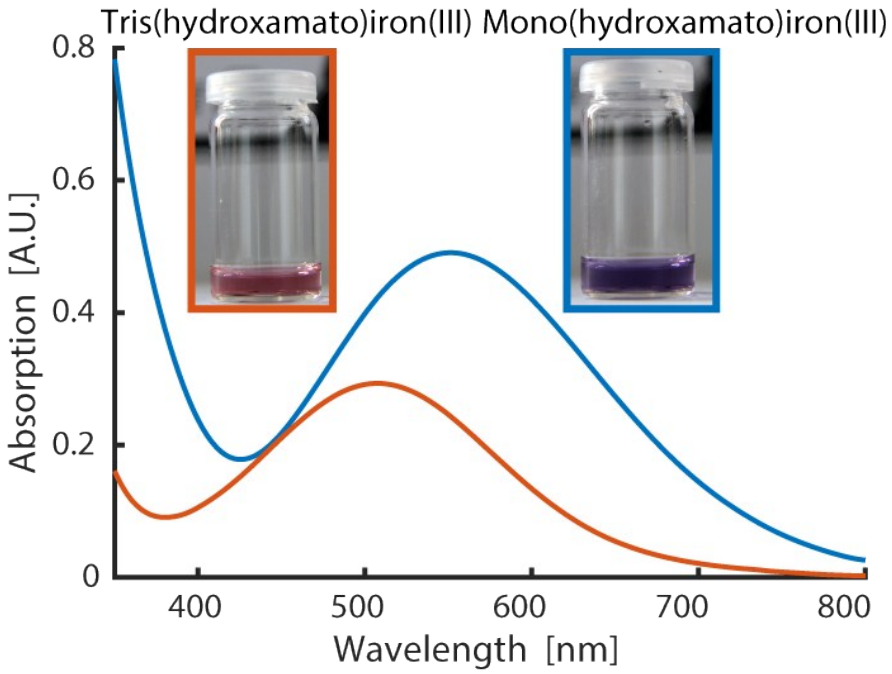

Figure S21. UV-Vis spectra of tris(HA-PEG)iron(III) (red) and mono(HA-PEG)iron(III) (blue) complexes in methanol.

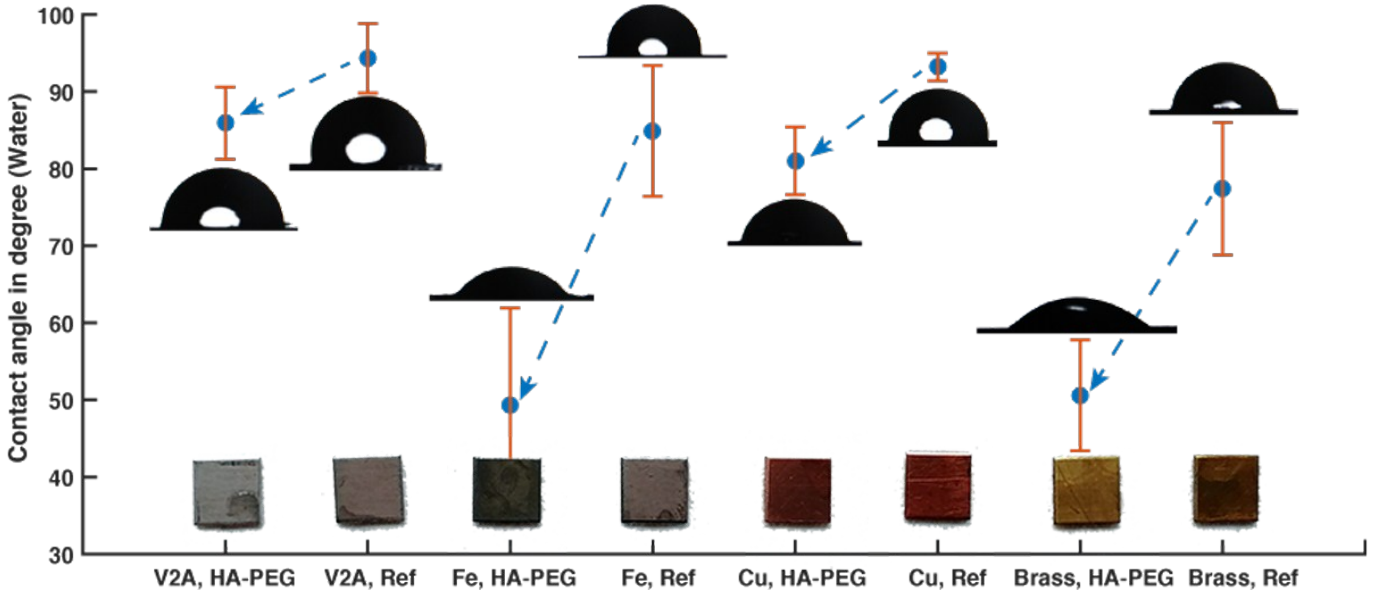

Figure S22. Contact angle measurements by the sessile drop method. PEG_{44} was used as a reference. In all cases, increased hydrophilicity of the corresponding surface was detected when HA-PEG_{188} was employed as a coating material.

Nanoparticle characterization

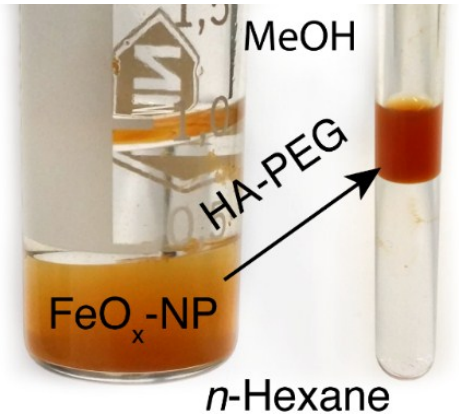

Figure S23. Proof of principle demonstration of the altered solubilisation behaviour of HA-PEG coated nanoparticles. Left image shows the non-modified nanoparticles solely soluble in *n*-hexane, while after coating with HA-PEG$_{188}$ the nanoparticles become freely soluble in methanol.

Table S1. Summary of DLS measurements.

Sample	Z_{avg} diameter [nm]	PDI	Peak diameter [nm]	Peak diameter standard deviation [nm]
NP-Oleat	20.9	0.10	21.3	4.5
NP-Oleat + PEG$_{44}$	22.2	0.10	23.7	6.7
NP-HA-PEG$_{21}$	25.8	0.08	27.1	6.5
NP-HA-PEG$_{80}$	35.8	0.07	38.9	9.7
NP-HA-PEG$_{188}$	49.4	0.09	53.4	12.3

T-Cell proliferation assay and MTT metabolic activity analysis

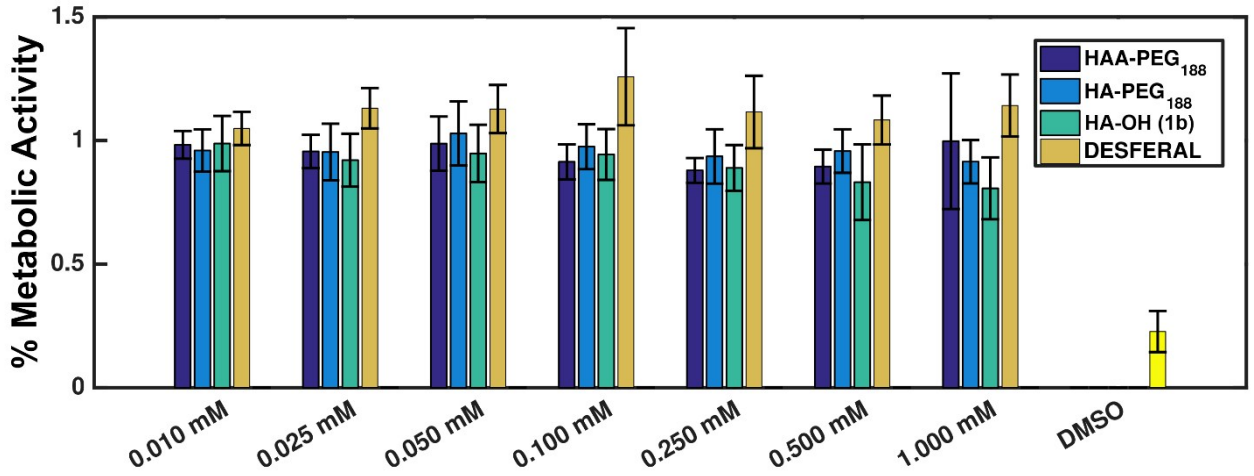

Figure S24. MTT metabolic activity assay. In all cases no significant decrease in metabolic activity, translating to cell toxicity can be observed. Only in case of low MW HA "HA-OH" (1b) a subtle decrease in metabolic activity was detected, suggesting increased toxicity compared to HA-PEG_{188}. (Data denote the mean±SEM of values obtained for PBMC prepared from 4 different healthy donors and tested in triplicates.)

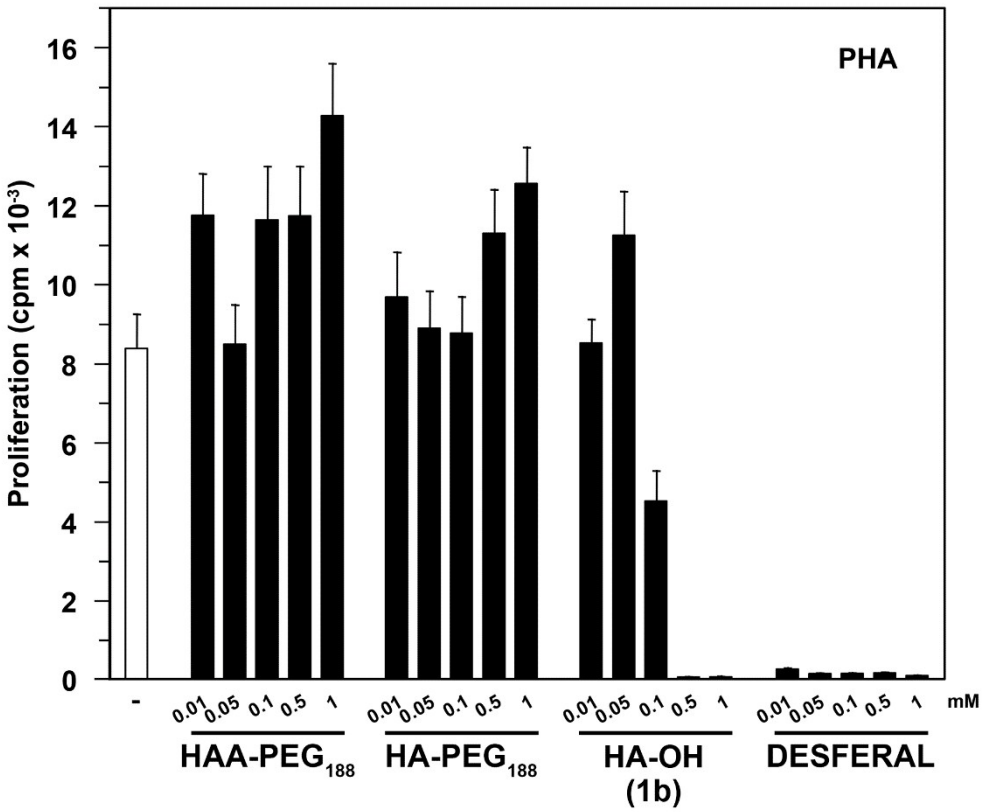

Figure S25. T-Cell proliferation assay. Human PBMC were stimulated with PHA to induce proliferation of T-cells in the presence of the different test compounds. In case of Desferal, proliferation was completely inhibited. Low MW HA compound "HA-OH" (1b) showed dose-dependent inhibition of proliferation. In contrast, no influence of HAA-PEG or HA-PEG was found regarding T-cell proliferation. (Data denote the mean±SEM of values obtained for PBMC prepared from 4 different healthy donors and tested in triplicates.)

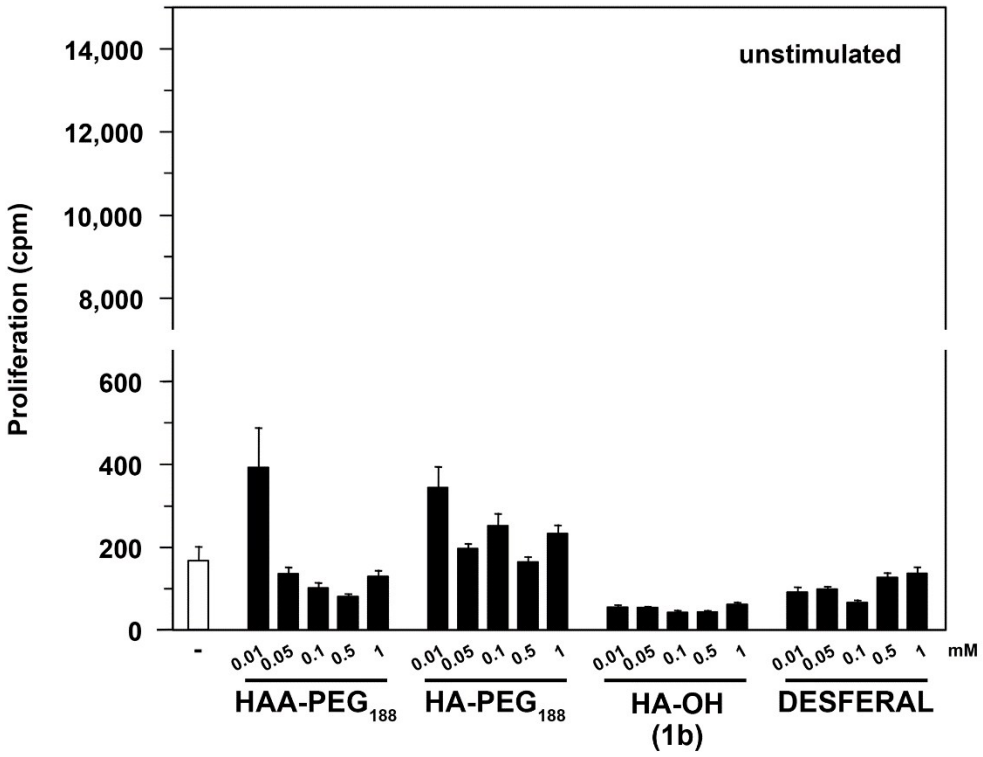

Figure S26. T-Cell proliferation assay. Unstimulated human PBMC were incubated with different test compounds. No significant effect towards background proliferation were found. (Data denote the mean±SEM of values obtained for PBMC prepared from 4 different healthy donors and tested in triplicates.)